

New Insights on Land Surface- Atmosphere Feedbacks over Tropical South America at Interannual Timescales

Juan Mauricio Bedoya-Soto & Germán Poveda

Universidad Nacional de Colombia, Sede Medellín

Departamento de Geociencias y Ambiente, Medellín, Colombia

First International Electronic Conference on the Hydrological Cycle,
SCIFORUM, 12–16 November 2017

Introduction

- Tropical South America (**TropSA**) concentrates a large amount of net radiation and water vapor.
- Intense heat and humidity fluxes dominate the interactions between soil and lower atmosphere.
- Soil moisture modulates diverse land-atmosphere feedbacks (**LAFs**); similarly, the rates of change between dry and wet conditions in the soil necessarily impact surface temperatures.

Introduction

- Interannual timescales are mainly controlled by ENSO (Trenberth et al., 1997, 2001, 2002, 2008; Wang, 1999, 2001; Wang et al., 2017).
- Known roles of land-surface interactions (Brubaker and Entekhabi, 1996; Koster et al., 2004; Xue et al., 2006; Bagley et al., 2014; Rocha et al., 2015; Ruscica et al., 2015; Kolstad et al., 2017; Zemp et al., 2017)

Introduction

Analysis of feedback mechanisms in land-atmosphere interaction

Kaye L. Brubaker¹ and Dara Entekhabi

Ralph M. Parsons Laboratory, Massachusetts Institute of Technology, Cambridge

Abstract. The initiation of a hydrologic drought may depend on large-scale or teleconnective causes; however, local positive feedbacks in the land-atmosphere system are believed to contribute to the observed persistence and intensification of droughts. In this study a basic linearization technique is combined with a nonlinear stochastic model of land-atmosphere interaction to analyze and, more importantly, quantify feedback mechanisms that arise in the coupled water and energy balances at the land surface. The model describes land-atmosphere interaction by four coupled stochastic ordinary differential equations in soil moisture, soil temperature, mixed-layer humidity, and mixed-layer potential temperature. The solution is a physically consistent joint probability distribution. The steady and perturbation-induced parts of the model equations are decomposed into the dependence of each component physical process upon each model state. Because of the negative correlation between soil moisture and soil temperature, the physical mechanisms that serve to restore each state individually (largely soil moisture control of evaporation and temperature dependence of saturation specific humidity) act as significant anomaly-reinforcing mechanisms for the other state.

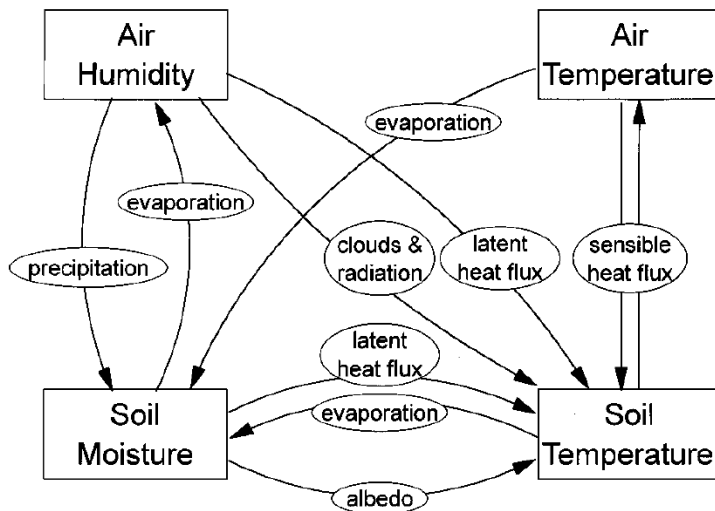


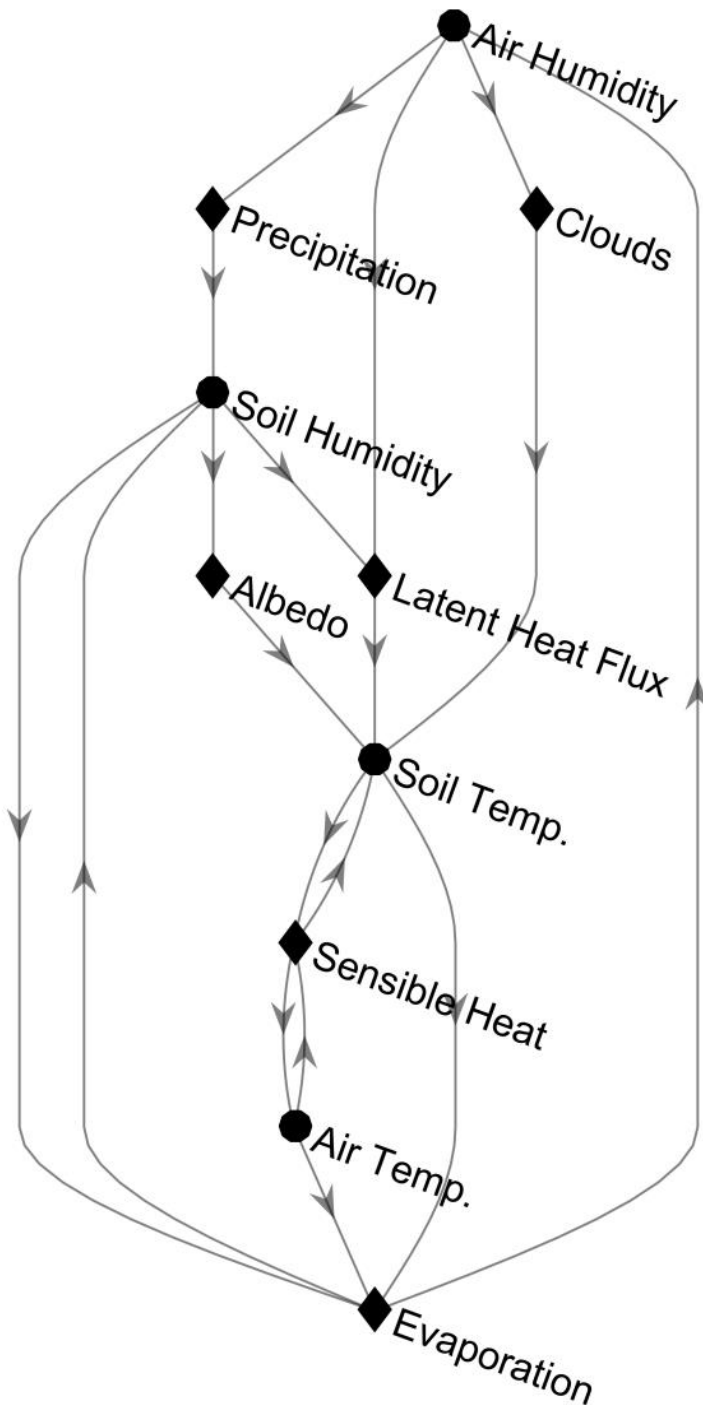
Figure 1. Conceptual diagram of well-known linkages among heat and moisture states in the soil and near-surface atmosphere.

Decomposition of the steady- and perturbation-forcing functions into the dependence of each component physical process upon each model state shows the following:

1. Soil moisture control of infiltration and of evaporation efficiency are self-restoring forces of comparable strength for the soil moisture state.
2. The temperature dependence of surface saturation specific humidity is a major factor in reinforcing soil moisture anomalies.
3. The individually strong, multiple (mostly radiative) effects of atmospheric humidity on ground temperature take opposite signs and cancel one another.
4. Soil moisture control of evaporation efficiency is the major mechanism by which the moisture state tends to reinforce temperature anomalies.
5. The temperature dependence of surface saturation specific humidity is a major self-restoring factor for the temperature state, and it exceeds the thermal radiation factor.
6. The buoyancy velocity is a significant recovery factor for temperature anomalies because it affects both the soil temperature and its coupling to air temperature. Soil temperature is positively correlated with temperature gradient anomalies; when the soil is anomalously warm, a strong gradient that enhances cooling also tends to be present.
7. Both the soil moisture and the soil temperature state are more susceptible to variations in wind speed (noise) when the system is dry than when it is moist.

It is well known that the soil moisture and soil temperature states are negatively correlated (cool/moist or warm/dry). These soil states communicate their covariability partially through local-scale interaction with the near-surface atmosphere. Because of the negative correlation between the states, the physical mechanisms that serve as restoring forces for each state individually (soil moisture control of evaporation and temperature dependence of saturation specific humidity) act as anomaly-enhancing positive feedback mechanisms for the other state. These feedback mechanisms are not apparent if the hydrologic variable soil moisture is considered alone. The coupled energy balance and energy states of the soil and near-surface atmosphere must be taken into account when seeking to understand and predict the persistence of hydrologic anomalies.

Links structure with Graph Theory



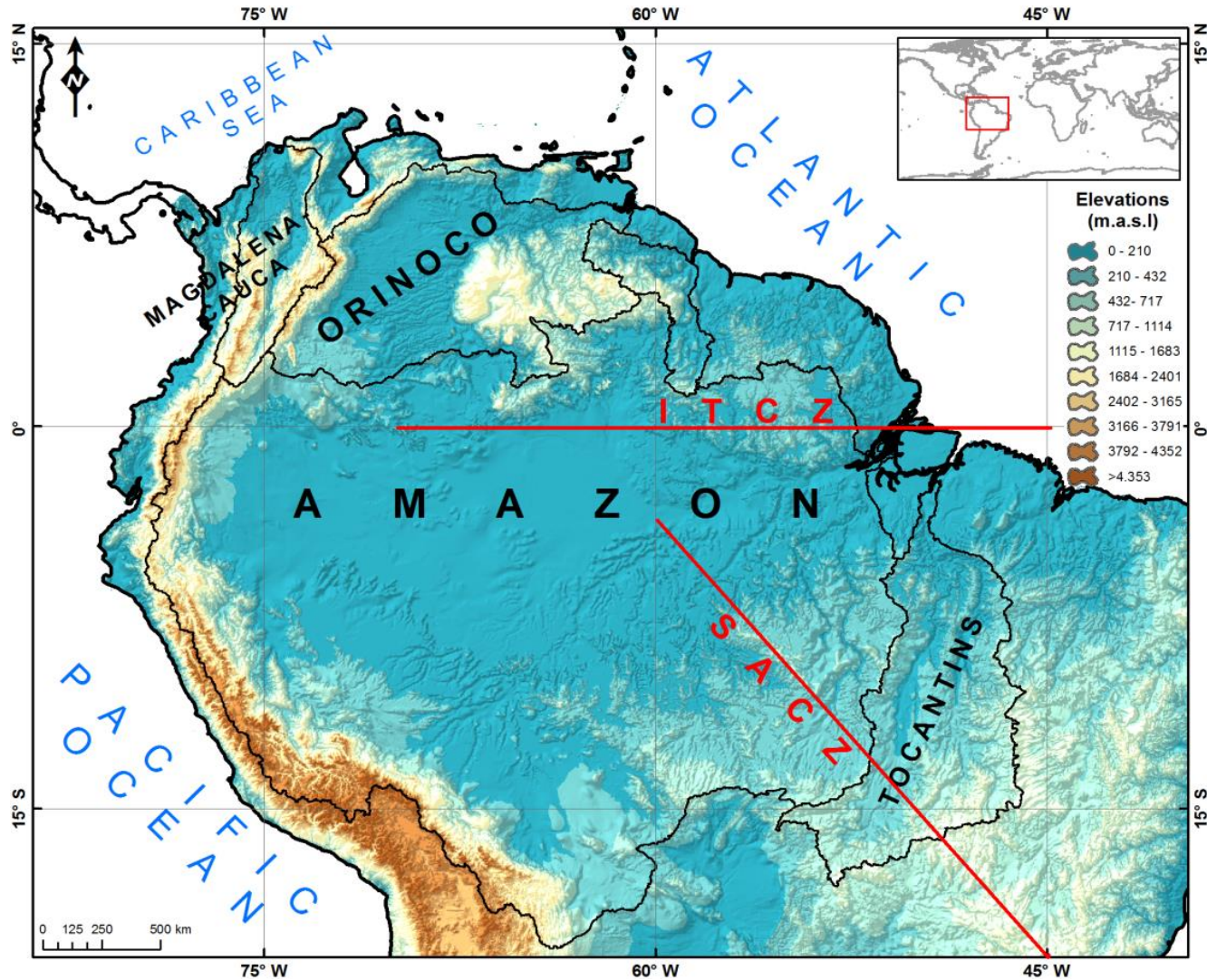
- Conceptual scheme of interconnections among the main variables involved in the studied land surface-atmosphere feedbacks (LAFs), adapted as a graph from Brubaker and Entekhabi (1996), and hierarchized by number of connections of each variable.
- The state (process) variables are denoted as circles (diamonds) nodes.
- Evaporation is the most heterogeneous process involved in LAFs since it connects soil humidity with the other state variables

Objectives

1. To study the essential role of Land Atmosphere Feedbacks and the mechanisms involved in water and heat anomalies in TropSA at interannual timescales.
2. To explore new tools to advance our understanding of land surface-atmospheric feedbacks in TropSA.
3. To integrate classical analyses of climatic fields with more recent methods of information theory and graph theory including linear and non-linear analysis.

Data and Methods

Study Region



Data

Visualize and Download GPCP Products



GPCP Product	Spatial Resolution	Time Coverage	Possible Application
First Guess Monthly	1.0°	2004 - present	drought monitoring
First Guess Daily	1.0°	2009 - present	analysis of extremes
Monthly Monitoring Version 5	1.0°, 2.5°	1982 - present	calibration of satellite data
Full Data Monthly Version 5	0.5°, 1.0°, 2.5°	1901 - 2013	hydrological studies
Full Data Daily Version 1	1.0°	1988 - 2013	analysis of extremes
HOAPS/GPCP global daily precipitation Version 1	0.5°, 1.0°, 2.5°	1988 - 2008	analysis of extremes
HOMPRA Europe Version 1 (coming soon)	1.0°	1951 - 2005	

Interim, Monthly Me x
ts/data/interim-full-mod/levtype=sfc/

n/LAND x
a/interim-land/type=an/

ECMWF

Home Chart dashboard Contact Search ECMWF Juan mauricio bedoya soto | Sign out

About Forecasts Computing Research Learning

Type of level

- Model levels
- Potential temperature
- Potential vorticity
- Pressure levels
- Surface

ERA Interim Fields

- Daily
- Invariant
- Synoptic Monthly Means
- Monthly Means of Daily Means
- Monthly Means of Daily Forecast Accumulations

About

- Conditions of use
- Documentation

Navigation

- Home
- Public Datasets
- Job list

See also...

- Access Public Datasets
- General FAQ
- WebAPI FAQ
- Accessing forecasts
- GRIB decoder

ERA Interim, Monthly Means of Daily Means

Please note that the fields shown on this interface are a subset of the ERA Interim dataset. The complete dataset (including wave fields) is available via the batch access. The full list of fields can be found [here](#).

Select a list of months

Year	Jan	Feb	Mar	Apr	May	Jun	Jul	Aug	Sep	Oct	Nov	Dec
1979	✓	✓	✓	✓	✓	✓	✓	✓	✓	✓	✓	✓
1981	✓	✓	✓	✓	✓	✓	✓	✓	✓	✓	✓	✓
1983	✓	✓	✓	✓	✓	✓	✓	✓	✓	✓	✓	✓
1985	✓	✓	✓	✓	✓	✓	✓	✓	✓	✓	✓	✓
1987	✓	✓	✓	✓	✓	✓	✓	✓	✓	✓	✓	✓
1989	✓	✓	✓	✓	✓	✓	✓	✓	✓	✓	✓	✓
1991	✓	✓	✓	✓	✓	✓	✓	✓	✓	✓	✓	✓
1993	✓	✓	✓	✓	✓	✓	✓	✓	✓	✓	✓	✓
1995	✓	✓	✓	✓	✓	✓	✓	✓	✓	✓	✓	✓
1997	✓	✓	✓	✓	✓	✓	✓	✓	✓	✓	✓	✓
1999	✓	✓	✓	✓	✓	✓	✓	✓	✓	✓	✓	✓
2001	✓	✓	✓	✓	✓	✓	✓	✓	✓	✓	✓	✓
2003	✓	✓	✓	✓	✓	✓	✓	✓	✓	✓	✓	✓
2005	✓	✓	✓	✓	✓	✓	✓	✓	✓	✓	✓	✓
2007	✓	✓	✓	✓	✓	✓	✓	✓	✓	✓	✓	✓
2009	✓	✓	✓	✓	✓	✓	✓	✓	✓	✓	✓	✓
2011	✓	✓	✓	✓	✓	✓	✓	✓	✓	✓	✓	✓
2013	✓	✓	✓	✓	✓	✓	✓	✓	✓	✓	✓	✓
2015	✓	✓	✓	✓	✓	✓	✓	✓	✓	✓	✓	✓

Select All or Clear

Select parameter

- 2 metre dewpoint temperature
- 10 metre U wind component
- 10 metre wind speed
- Boundary layer height
- Convective available potential energy
- 2 metre temperature
- 10 metre V wind component
- Albedo
- Charnock
- Forecast albedo

ECMWF

Home Chart dashboard Contact Search ECMWF Juan mauricio bedoya soto | Sign out

About Forecasts Computing Research Learning

ERA Interim/LAND

Select date

Select a date in the interval 1979-01-01 to 2010-12-31

Start date: 1979-01-01 End date: 2010-12-31

Select a list of months

Year	Jan	Feb	Mar	Apr	May	Jun	Jul	Aug	Sep	Oct	Nov	Dec
1979	✓	✓	✓	✓	✓	✓	✓	✓	✓	✓	✓	✓
1981	✓	✓	✓	✓	✓	✓	✓	✓	✓	✓	✓	✓
1983	✓	✓	✓	✓	✓	✓	✓	✓	✓	✓	✓	✓
1985	✓	✓	✓	✓	✓	✓	✓	✓	✓	✓	✓	✓
1987	✓	✓	✓	✓	✓	✓	✓	✓	✓	✓	✓	✓
1989	✓	✓	✓	✓	✓	✓	✓	✓	✓	✓	✓	✓
1991	✓	✓	✓	✓	✓	✓	✓	✓	✓	✓	✓	✓
1993	✓	✓	✓	✓	✓	✓	✓	✓	✓	✓	✓	✓
1995	✓	✓	✓	✓	✓	✓	✓	✓	✓	✓	✓	✓
1997	✓	✓	✓	✓	✓	✓	✓	✓	✓	✓	✓	✓
1999	✓	✓	✓	✓	✓	✓	✓	✓	✓	✓	✓	✓
2001	✓	✓	✓	✓	✓	✓	✓	✓	✓	✓	✓	✓
2003	✓	✓	✓	✓	✓	✓	✓	✓	✓	✓	✓	✓
2005	✓	✓	✓	✓	✓	✓	✓	✓	✓	✓	✓	✓
2007	✓	✓	✓	✓	✓	✓	✓	✓	✓	✓	✓	✓
2009	✓	✓	✓	✓	✓	✓	✓	✓	✓	✓	✓	✓

Select All or Clear

Select time

00:00:00 06:00:00 12:00:00 18:00:00

Select parameter

- Skin temperature
- Soil temperature level 1
- Temperature of snow layer
- Volumetric soil water layer 4
- Snow albedo
- Soil temperature level 2
- Volumetric soil water layer 1
- Snow density
- Soil temperature level 3
- Volumetric soil water layer 2
- Snow depth
- Soil temperature level 4
- Volumetric soil water layer 3

Select All or Clear

View the MARS request Retrieve GRIB Retrieve NetCDF

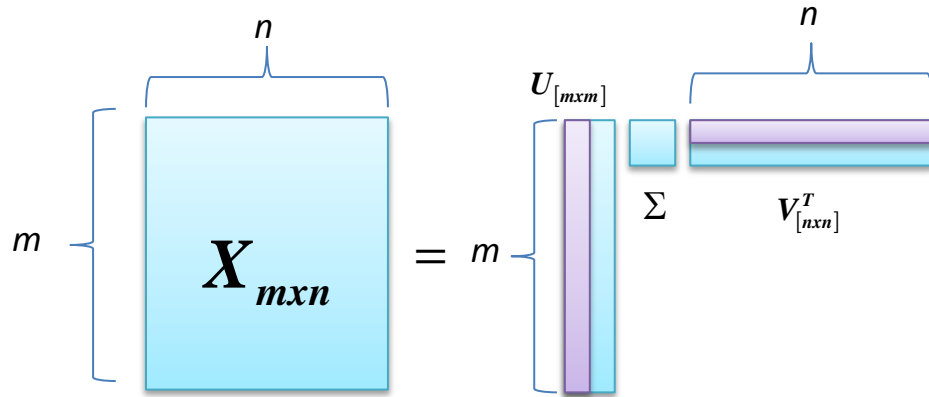
Data

- **Soil moisture** (VSW) from Era-Interim
Land $1^{\circ} \times 1^{\circ}$
- **Specific Humidity at 925 hPa** (SH^{925}), **2m Temperature** (T_{2m}) and **Evaporation** (EVP)
from ERA-Interim $1^{\circ} \times 1^{\circ}$
- **Precipitation** (PRC) from GPCC $1^{\circ} \times 1^{\circ}$
- All climate fields period 1979-2010

Methods

- **SVD, Entropy, and Noise Reduction:** After standardized each variable and apply a Singular Value Decomposition (SVD), we select the representative modes of each variable at interannual time scale (noise reduction) using a criterion from the information theory (Entropy). 5 variables denoised.
- **Maximum Covariance Analysis of Interannual Variability in TropSA:** We apply a SVD on the covariance matrices thus establishing connections between all possible pairs of variables (10 possible combinations)
- **Graph Models of LAF in Tropical South America at Interannual Timescales:** Establishing connections among variables and defining relationship structure. We use linear and non-linear metrics as links.

SVD, Noise Reduction, and Entropy



X is the standardized time-space matrix for each variable

$$X_{m \times n} = U_{[m \times m]} \Sigma_{[m \times n]} V_{[n \times n]}^T$$

$$X_{m \times n} = U_{[m \times m]} \Sigma_{[m \times n]} V_{[n \times n]}^T = \sum_{i=1}^{\min(m,n)} u_i \sigma_i v_i^T = u_1 \sigma_1 v_1^T + u_2 \sigma_2 v_2^T + \dots + u_m \sigma_m v_m^T$$

Truncated matrix of lower rank k

$$X \approx \hat{X}_{m \times n} = U_{[m \times k]} \Sigma_{[k \times k]} V_{[n \times k]}^T = \sum_{i=1}^k u_i \sigma_i v_i^T = u_1 \sigma_1 v_1^T + u_2 \sigma_2 v_2^T + \dots + u_k \sigma_k v_k^T \text{ con } k < r$$

Relative contribution of each singular factor

$$f_i = \sigma_i^2 / \sum_i \sigma_i^2$$

$$H_X = -\frac{1}{\log_2(\min\{n,m\})} \sum_{i=1}^{\min(n,m)} f_i \log_2 f_i$$

Entropy for each matrix k

Cummulated contribution

$$F_i = \sum_i f_i$$

$$\min(k) \rightarrow \sum_{i=1}^k f_i \geq E$$

Entropy criterion to select k and noise reduction

Maximum Covariance Analysis (MCA) with Interannual Variability in TropSA

Covariance matrix

$$C_{XY} = \frac{1}{n-1} \hat{X}\hat{Y}^T$$

$$f_k^{XY} = \sigma_k^2 / \sum_i \sigma_i^2$$

Square covariance fraction of the k-factor of the MCA

$$C_{XY [mxq]} = U_{[mxk]} \Sigma_{[kxk]} V_{[qyk]}^T = \sum_{i=1}^k u_i \sigma_i v_i^T$$

$$x_k = u_k^T \hat{X}$$

Expansion coefficients

$$y_k = v_k^T \hat{Y}$$

- The SVD of couple fields (MCA) identify only modes in which those are strongly coupled
- Converts a set of correlated variables to visualize the relationships between them
- Identify and order the dimensions where the data exhibit the greatest covariability
- Better approximation to the data using less dimensions

We use the first $k=3$ Maximum Covariance States (**MCS_k**) to characterize the cumulative covariance and its space-time distribution

As a result we obtain 4 kind of maps

Symbol	Description of map
$\rho(x_k, \hat{Y})$	Correlation between vector x_k with each column vector of matrix \hat{Y}
$\rho(y_k, \hat{X})$	Correlation between vector y_k with each column vector of matrix \hat{X}
$\rho(x_k, \hat{X})$	Correlation between vector x_k with each column vector of matrix \hat{X}
$\rho(y_k, \hat{Y})$	Correlation between vector y_k with each column vector of matrix \hat{Y}

Non-Linear Dependence: Causality (Liang 2013, 2014, 2015)

The Liang-Kleeman information flow: Theory and applications

XS Liang - Entropy, 2013 - mdpi.com

Abstract: Information flow, or information transfer as it may be referred to, is a fundamental notion in general physics which has wide applications in scientific disciplines. Recently, a rigorous formalism has been established with respect to both deterministic and stochastic

↻ Cited by 20 Related articles All 10 versions ↻

Unraveling the cause-effect relation between time series

X San Liang - Physical Review E, 2014 - APS

Abstract Given two time series, can one faithfully tell, in a rigorous and quantitative way, the cause and effect between them? Based on a recently rigorized physical notion, namely, information flow, we solve an inverse problem and give this important and challenging

↻ Cited by 31 Related articles All 7 versions

Normalizing the causality between time series

X San Liang - Physical Review E, 2015 - APS

Abstract Recently, a rigorous yet concise formula was derived to evaluate information flow, and hence the causality in a quantitative sense, between time series. To assess the importance of a resulting causality, it needs to be normalized. The normalization is achieved

↻ Cited by 5 Related articles All 12 versions

PHYSICAL REVIEW E 90, 052150 (2014)

Unraveling the cause-effect relation between time series

X. San Liang*

School of Marine Sciences, Nanjing University of Information Science and Technology (Nanjing Institute of Meteorology), Nanjing 210044 and China Institute for Advanced Study, Central University of Finance and Economics, Beijing 100081, China
(Received 8 June 2014; revised manuscript received 14 October 2014; published 24 November 2014)

Given two time series, can one faithfully tell, in a rigorous and quantitative way, the cause and effect between them? Based on a recently rigorized physical notion, namely, information flow, we solve an inverse problem and give this important and challenging question, which is of interest in a wide variety of disciplines, a positive answer. Here causality is measured by the time rate of information flowing from one series to the other. The resulting formula is tight in form, involving only commonly used statistics, namely, sample covariances; an

The rate of information (causality) flowing from a component, say, Y, to another, say, X, is the change rate of the marginal entropy of X, minus the same change rate but with the effect from Y instantaneously excluded from the system.

Absolute Causality formula:

$$T_{Y \rightarrow X} = \frac{C_{xx} C_{xy} C_{y,dx} - C_{xy}^2 C_{x,dy}}{C_{xx}^2 C_{yy} - C_{xx} C_{xy}^2}$$

where C_{xx} , C_{xy} y C_{yy} denote the possible covariances between series.

Relative Causality (τ)

PHYSICAL REVIEW E 92, 022126 (2015)

Normalizing the causality between time series

X. San Liang*

Nanjing University of Information Science and Technology (Nanjing Institute of Meteorology), Nanjing 210044, and China Institute for Advanced Study, Central University of Finance and Economics, Beijing 100081, China

(Received 18 January 2015; revised manuscript received 31 May 2015; published 17 August 2015)

Recently, a rigorous yet concise formula was derived to evaluate information flow, and hence the causality in a quantitative sense, between time series. To assess the importance of a resulting causality, it needs to be normalized. The normalization is achieved through distinguishing a Lyapunov exponent-like, one-dimensional phase-space stretching rate and a noise-to-signal ratio from the rate of information flow in the balance of the marginal entropy evolution of the flow recipient. It is verified with autoregressive models and applied to a real financial analysis problem. An unusually strong one-way causality is identified from IBM (International Business Machines Corporation) to GE (General Electric Company) in their early era, revealing to us an old story, which has almost faded into oblivion, about “Seven Dwarfs” competing with a giant for the mainframe computer market.

$$Z_{y \rightarrow x} = |T_{y \rightarrow x}| + \left| \frac{dH_y^*}{dt} \right| + \left| \frac{dH_y^{noise}}{dt} \right|$$

Marginal entropy

p and q are maximum likelihood estimators of Z

$$p = \frac{C_{yy}C_{x,dx} - C_{xy}C_{y,dx}}{\det(C)}$$

$$q = \frac{C_{yy}C_{x,dx} - C_{xy}C_{y,dx}}{\det(C)}$$

Relative Flow of Information or Relative causality

$$\tau_{y \rightarrow x} = \frac{|Z_{y \rightarrow x}|}{T_{y \rightarrow x}} * 100$$

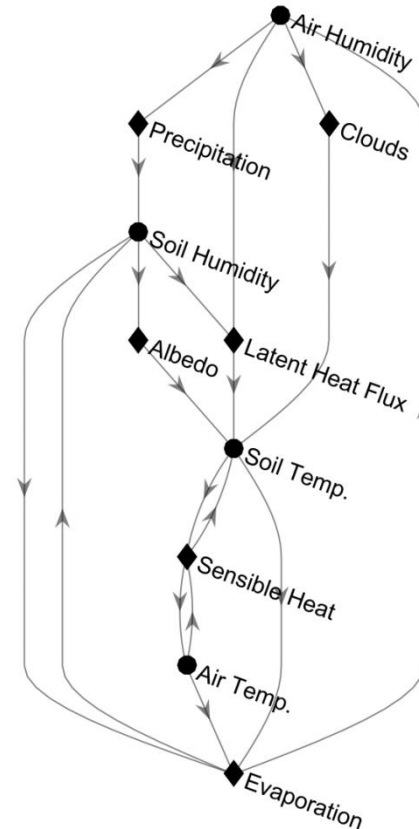
If the result is 100, x is 100% due to the flow of information from y .

$$\left| \frac{dH_y^*}{dt} \right| = p$$

$$\left| \frac{dH_y^{noise}}{dt} \right| = \frac{\Delta t}{2C_{xx}} (C_{dx,dx} + p^2 C_{xx} + q^2 C_{yy} - 2pC_{dx,x} - 2qC_{dx,y} + 2pqC_{xy})$$

Graph Theory

- Time series extracted from the MCA procedures were used to quantify linear (correlations) and nonlinear (causalities) metrics for different time lags among all pairs of variables.
- All sets of associations were summarized in the form of correlation and causality graphs in turn grouped according to their association degree with ENSO.
- This way, we analyzed how the LAFs over TropSA contribute to explain the simultaneous and lagged interannual anomalies over land and atmosphere.
- We also applied spectral analysis to infer links structure at each lag as a graph using the adjacency matrix



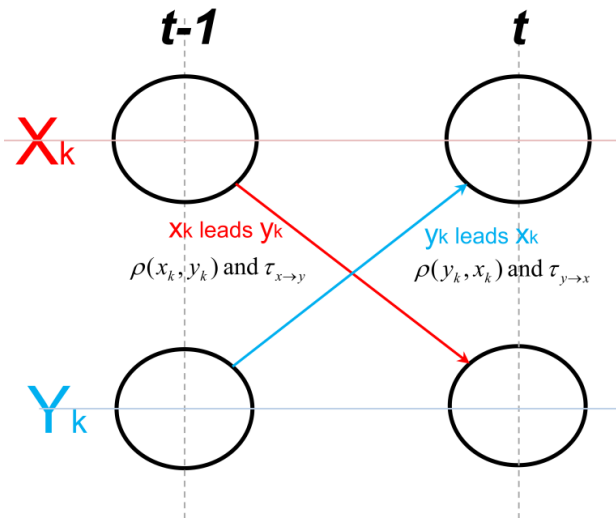
Authoritative sources in a hyperlinked environment

[JM Kleinberg](#) - Journal of the ACM (JACM), 1999 - dl.acm.org

Abstract The network structure of a hyperlinked environment can be a rich source of information about the content of the environment, provided we have effective means for understanding it. We develop a set of algorithmic tools for extracting information from the link structures of such environments, and report on experiments that demonstrate their effectiveness in a variety of context on the World Wide Web. The central issue we address ...

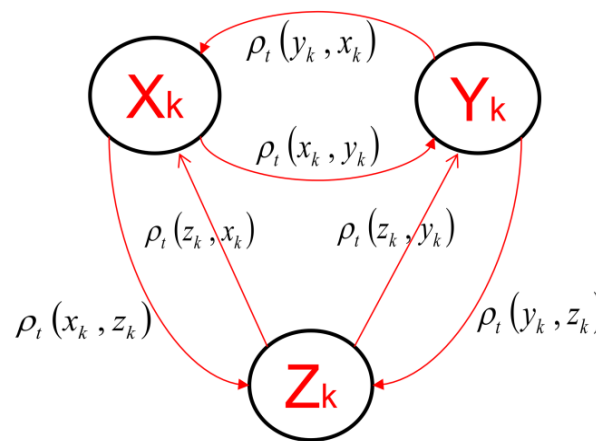
☆ 77 Cited by 8517 Related articles All 194 versions

Adjacency Matrix of a Graph (Linear and Non-Linear Metrics as Edges)

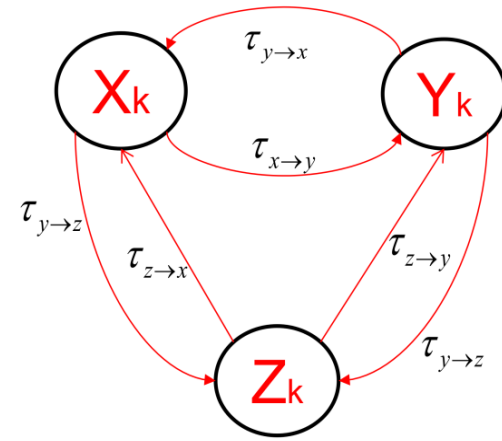


Basic scheme of the interaction between two singular vectors resulting from a Maximum Covariance Analysis (MCA) between two variables X and Y for each mode k assuming 1 lag-month

Graphs among three variables (X, Y, Z) with links denoting lagged correlations (top left) and causalities (top right) between variables/nodes.



ρ_t : Significant Correlations ($P < 1\%$)
 $t = 1$ to 9 months lag



τ : Causalities
 $t = 1$ to 9 months lag

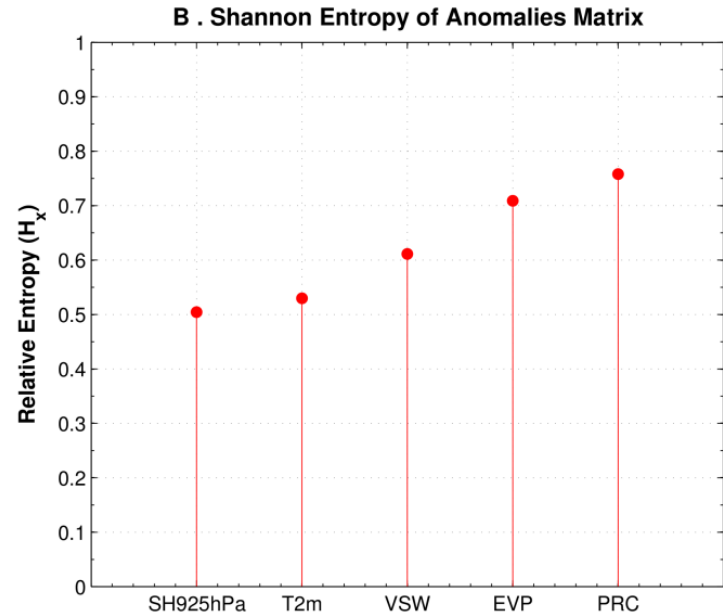
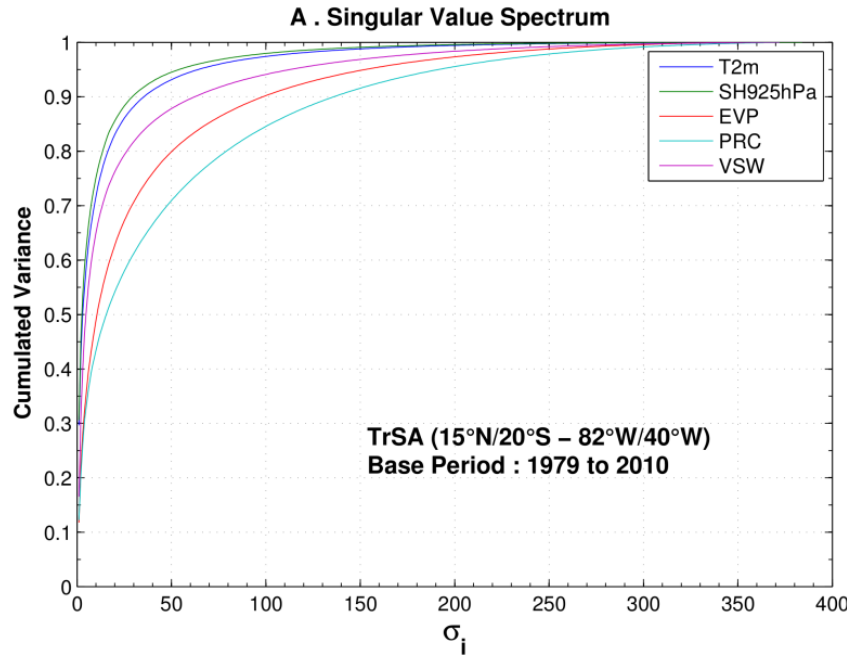
Bottom panels include the structure of the graph's adjacency matrix, W, to illustrate the node-to-node connection that is established in each graph.

$$W_{[ij]}^\rho = \begin{matrix} & X & Y & Z \\ X & \begin{pmatrix} 0 & \rho_t(x_k, y_k) & \rho_t(x_k, z_k) \end{pmatrix} \\ Y & \begin{pmatrix} \rho_t(y_k, x_k) & 0 & \rho_t(y_k, z_k) \end{pmatrix} \\ Z & \begin{pmatrix} \rho_t(z_k, x_k) & \rho_t(z_k, y_k) & 0 \end{pmatrix} \end{matrix}$$

$$W_{[ij]}^\tau = \begin{matrix} & X & Y & Z \\ X & \begin{pmatrix} 0 & \tau_{x \rightarrow y} & \tau_{x \rightarrow z} \end{pmatrix} \\ Y & \begin{pmatrix} \tau_{y \rightarrow x} & 0 & \tau_{y \rightarrow z} \end{pmatrix} \\ Z & \begin{pmatrix} \tau_{z \rightarrow x} & \tau_{z \rightarrow y} & 0 \end{pmatrix} \end{matrix}$$

Results

Noise Reduction



Data Source	$X_{m \times n}$	m (# of cells 1°)	n (# months)	$rank(X)$	f_1	f_2	H_x	k_H	f_{k_H}
GPCC	Precipitation (PRC)	1101	384	372	0.12	0.20	0.76	64	0.76
ERA-Interim	Evaporation (EVP)	1047		372	0.12	0.22	0.71	31	0.71
ERA-Interim Land	Volumetric Soil Water Content (VSW)	1039		348	0.16	0.31	0.61	9	0.63
ERA-Interim	Air Temperature (T_{2m})	1047		348	0.30	0.43	0.53	4	0.55
ERA-Interim	Specific Humidity at 925 hPa (SH^{925})	1047		348	0.31	0.45	0.50	3	0.53

- A matrix X with low relative entropy (H_x) represents a variable controlled by few modes over TropSA at interannual timescales.
- State atmospheric variables SH^{925} and T_{2m} are the less complex variables of our datasets (64 and 31 k_H factors)
- Process variables (PRC and EVP) are the most

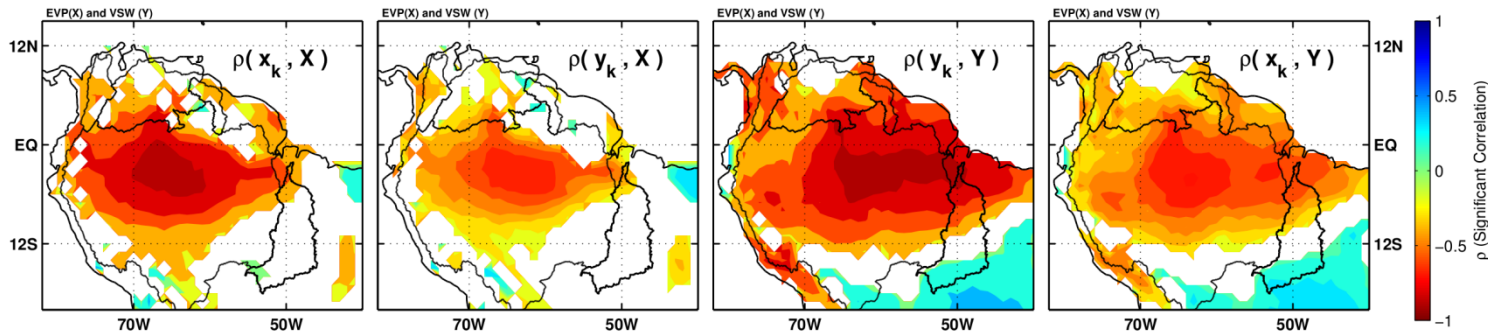
MCA over TropSA

C_{XY}		EMC_1		EMC_2		EMC_3		H_{XY}
\hat{X}	\hat{Y}	$f_1^{XY} (F_1^{XY})$	$\rho(x_1, y_1)$	$f_2^{XY} (F_2^{XY})$	$\rho(x_2, y_2)$	$f_3^{XY} (F_3^{XY})$	$\rho(x_3, y_3)$	
SH⁹²⁵	T_{2m}	0.78 (0.78)	0.95	0.16 (0.94)	0.96	0.06 (1.00)	0.94	0.09
EVP	T_{2m}	0.64 (0.64)	0.54	0.23 (0.87)	0.63	0.08 (0.95)	0.53	0.14
PRC	SH⁹²⁵	0.63 (0.63)	0.75	0.29 (0.92)	0.51	0.08 (1.00)	0.49	0.12
EVP	VSW	0.59 (0.59)	0.76	0.18 (0.77)	0.62	0.12 (0.89)	0.61	0.18
EVP	SH⁹²⁵	0.59 (0.59)	0.52	0.31 (0.90)	0.60	0.10 (1.00)	0.51	0.13
PRC	T_{2m}	0.59 (0.59)	0.69	0.32 (0.91)	0.54	0.06 (0.97)	0.50	0.13
SH⁹²⁵	VSW	0.58 (0.58)	0.67	0.36 (0.94)	0.50	0.06 (1.00)	0.38	0.12
T_{2m}	VSW	0.57 (0.57)	0.62	0.33 (0.90)	0.55	0.06 (0.96)	0.55	0.14
EVP	PRC	0.42 (0.42)	0.70	0.34 (0.76)	0.72	0.11 (0.87)	0.70	0.23
PRC	VSW	0.41 (0.41)	0.77	0.36 (0.75)	0.77	0.08 (0.88)	0.78	0.20

- Set of reduced variables over TropSA (Table) to derive all possible pairs of truncated matrices for a crosslink analysis.
- We estimate a total of 10 covariance matrices
- The first $k=3$ MCS_k characterize more than 85% of the cumulative covariance of each covariance matrix

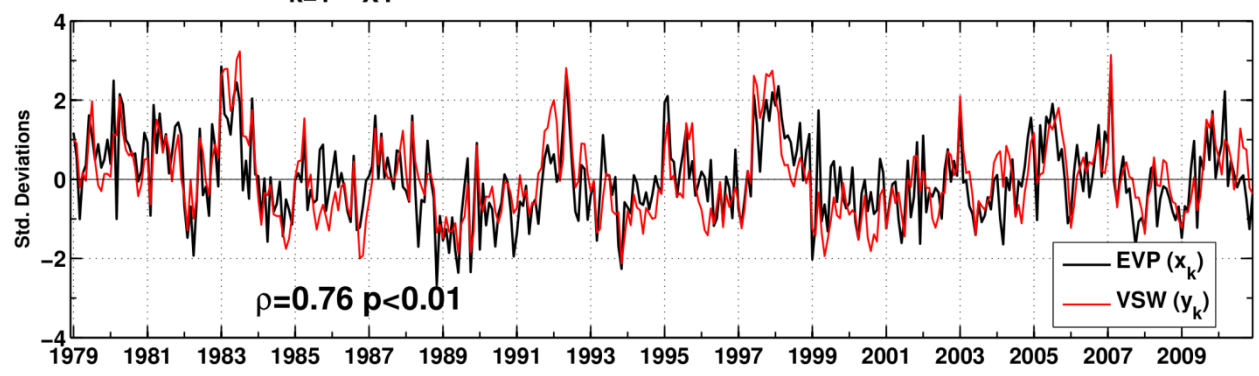
- T_{2m} - SH⁹²⁵ (both state variables) has the to 78% of its total covariance in the first relative fraction
- PRC-EVP (42 %) and PRC-VSW (41 %) concentrate the lowest fraction in the first relative fraction

MCA_{k=1} of X = EVP & Y = VSW $f_{XY1} = 58.68\%$ – Correlation Maps (P<1%) – 1979:2010

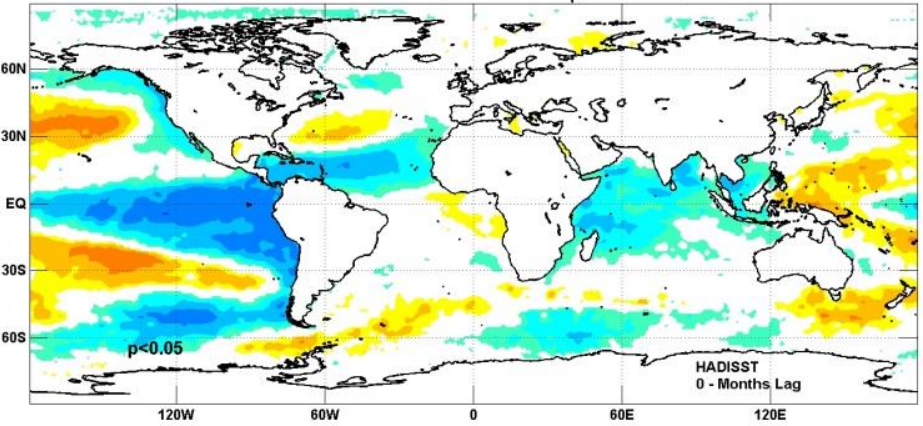


The core of interannual interactions of soil humidity and evaporation is located in the Amazon River basin, in connection with the Magdalena-Cauca River basin over north-western TropSA

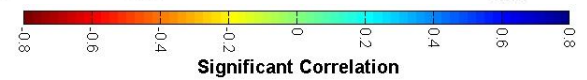
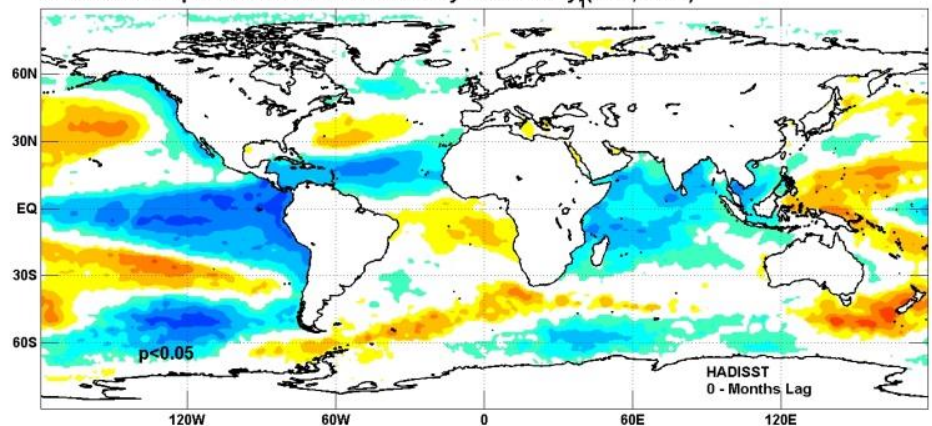
MCA_{k=1} ($f_{XY} = 58.68\%$) of EVP & VSW (15N/20S – 82W/40W)



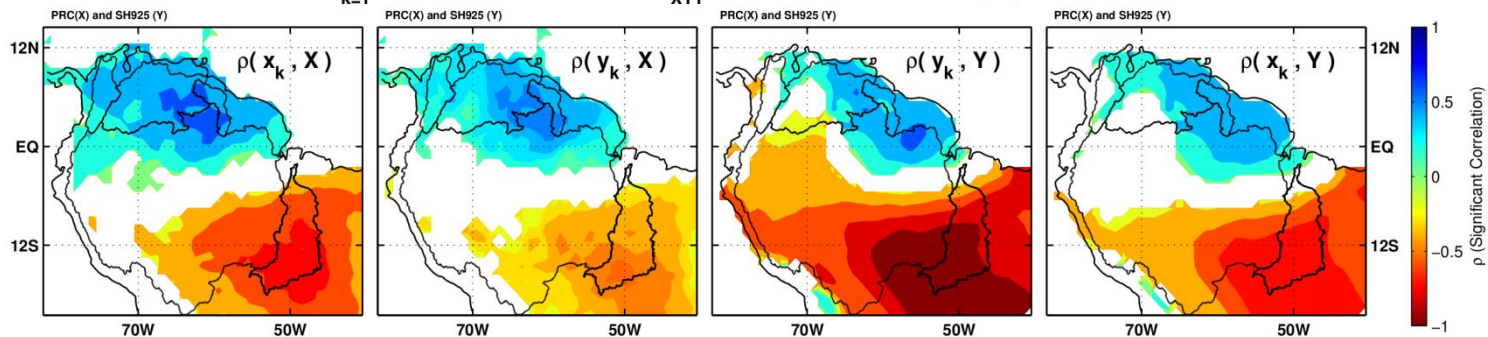
Correlation map 1979:2010 of mean monthly SSTs with x_1 (EVP, VSW)



Correlation map 1979:2010 of mean monthly SSTs with y_1 (EVP, VSW)

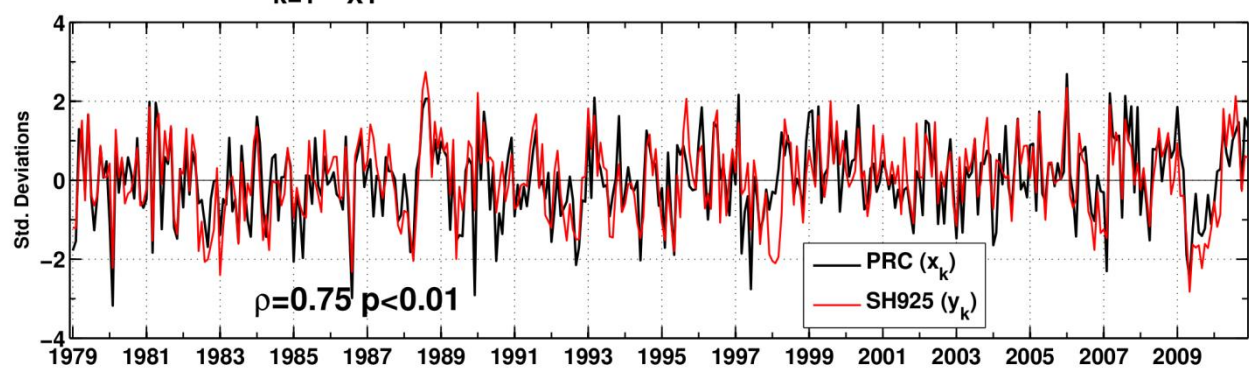


MCA_{k=1} of X = PRC & Y = SH925 $f_{XY1}=63.15\%$ - Correlation Maps (P<1%)- 1979:2010

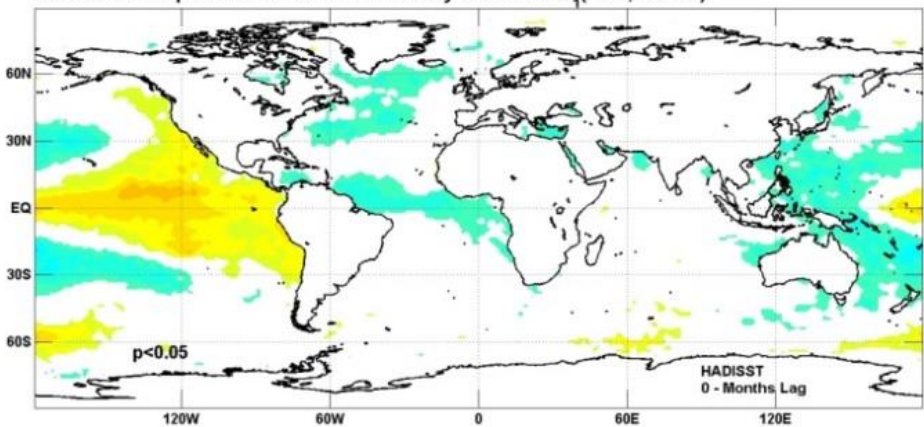


The spatial correlation pattern associated with this pair of variables (MCS₁ of SH⁹²⁵-PRC) exhibits a dipole with one center in the northwest (direct correlations), and other in the southeast (inverse).

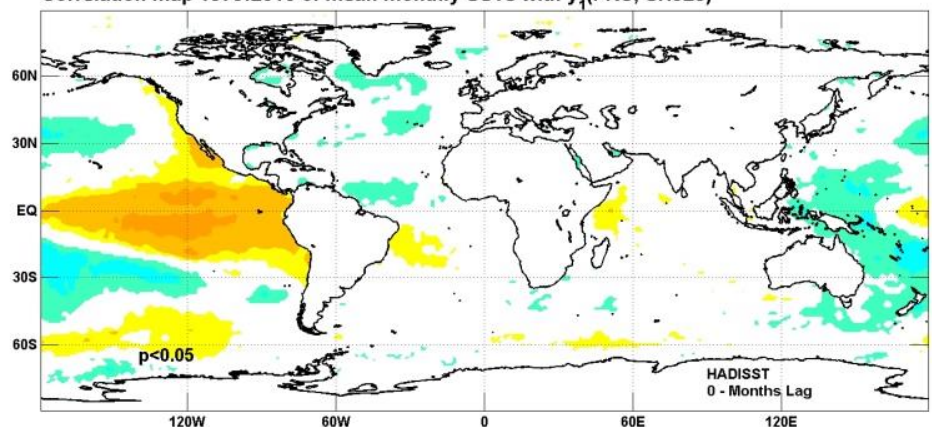
MCA_{k=1} ($f_{XY} = 63.15\%$) of PRC & SH925 (15N/20S - 82W/40W)



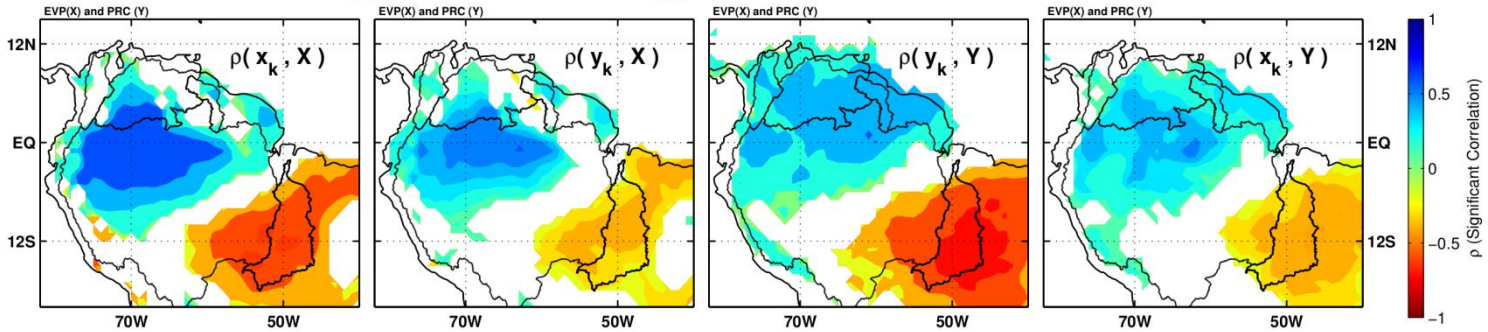
Correlation map 1979:2010 of mean monthly SSTs with x_1 (PRC, SH925)



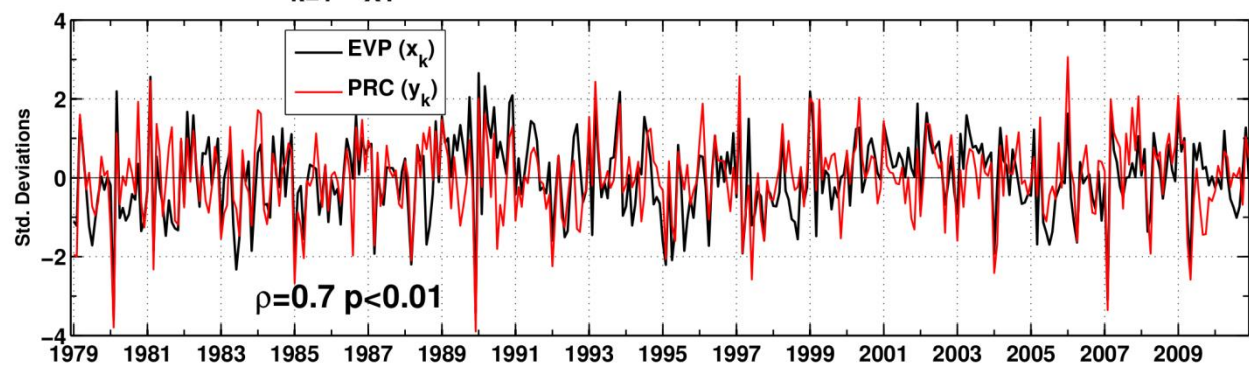
Correlation map 1979:2010 of mean monthly SSTs with y_1 (PRC, SH925)



MCA_{k=1} of X = EVP & Y = PRC f_{XY1}=41.56% - Correlation Maps (P<1%)- 1979:2010

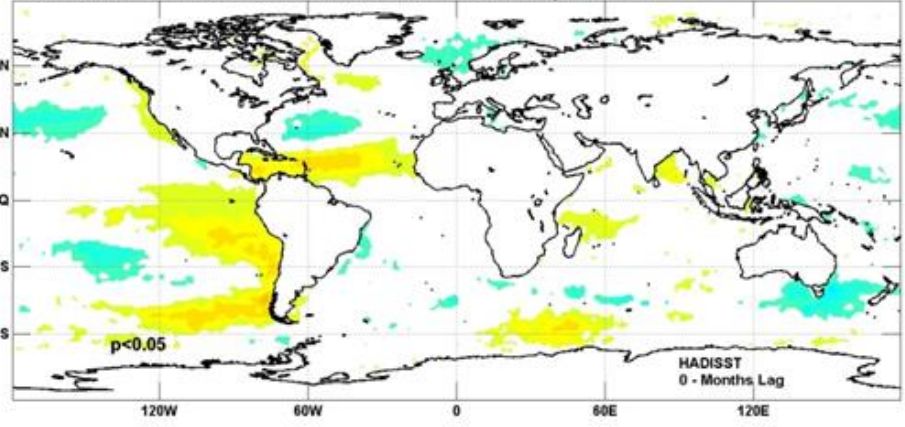


MCA_{k=1} (f_{XY} = 41.56%) of EVP & PRC (15N/20S - 82W/40W)

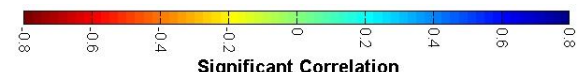
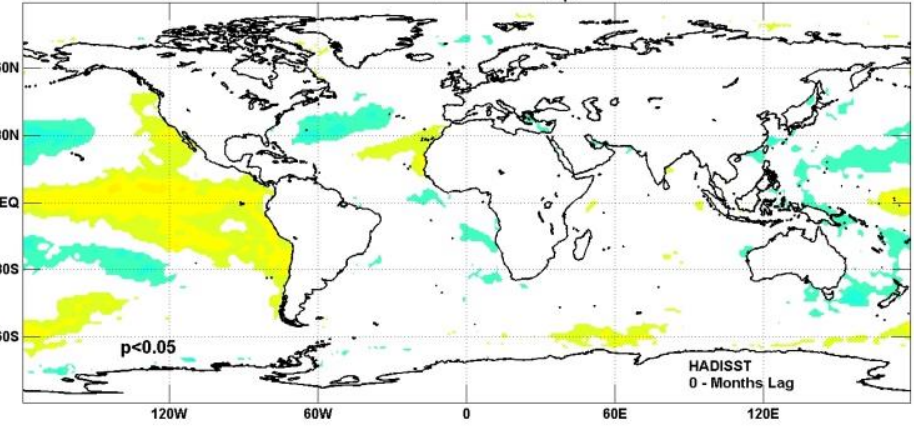


Correlations over the northern pole of the MCS1 of PRC-EVP are significant over the piedmont of Amazon-Orinoco River basins.

Correlation map 1979:2010 of mean monthly SSTs with x_1 (EVP, PRC)



Correlation map 1979:2010 of mean monthly SSTs with y_1 (EVP, PRC)



Results (2)

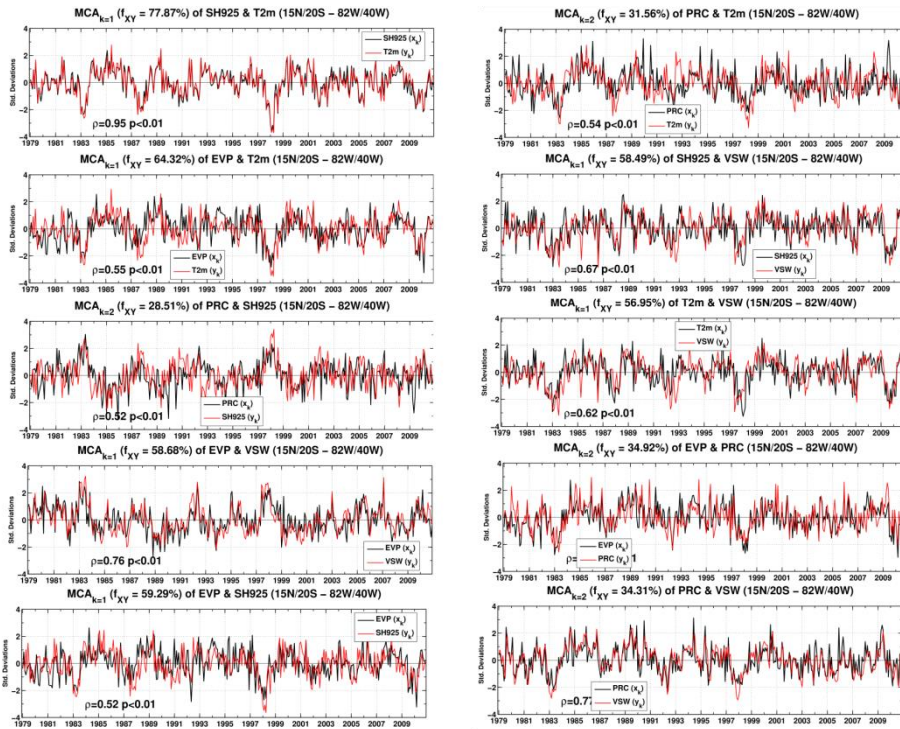
Graphs with Linear Edges

ENSO-intensities Categorizing Interannual Oceanic Modes

C_{XY}		MCS ₁		MCS ₂		MCS ₃	
\hat{X}	\hat{Y}	$\rho(x_1, N3.4)$	$\rho(y_1, N3.4)$	$\rho(x_2, N3.4)$	$\rho(y_2, N3.4)$	$\rho(x_3, N3.4)$	$\rho(y_3, N3.4)$
SH ⁹²⁵	T _{2m}	-0.44	-0.50	0.15	0.13	-0.20	-0.17
EVP	T _{2m}	-0.48	-0.52	0.11	0.12	0.14	0.14
PRC	SH ⁹²⁵	-0.25	-0.31	0.40	0.45	-0.20	0.10
EVP	VSW	0.4	0.44	0.32	0.36	0.11	0.18
EVP	SH ⁹²⁵	-0.44	-0.44	0.20	0.21	0.22	0.05
PRC	T _{2m}	0.32	0.43	-0.32	-0.45	-0.17	0.03
SH ⁹²⁵	VSW	-0.43	-0.47	0.36	0.35	-0.10	-0.03
T _{2m}	VSW	-0.52	-0.55	-0.30	-0.21	-0.05	-0.09
EVP	PRC	-0.08	-0.19	-0.48	-0.4	-0.22	-0.31
PRC	VSW	0.3	0.37	-0.35	-0.4	0.21	0.21

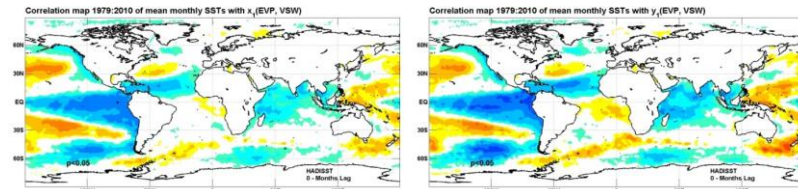
- Correlation between MCA series and Niño 3.4 index, for the MCS_k, k=1,2, and 3.
- High correlation values are denoted in blue, medium values in green and low values in red.

A. High ENSO-related MCS₁(EVP, VSW) $f_1^{XY} = 59\%$

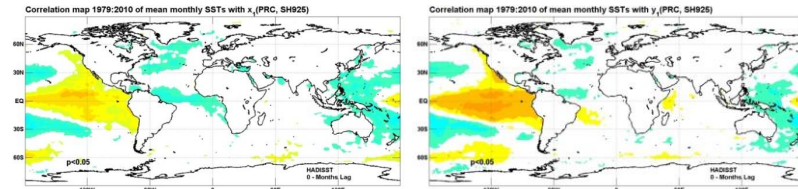


Left: Expansion coefficients for all possible combinations as pairs among VSW, SH925, T2m, EVP and PRC

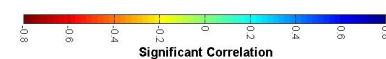
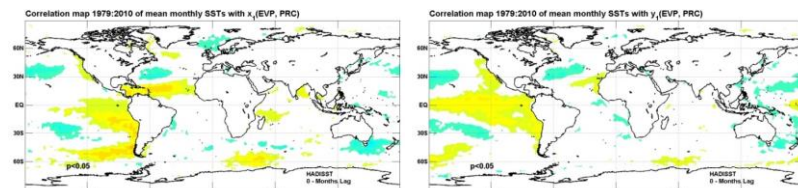
Right: Correlations expansion coefficients x_k and y_k with SSTs from HADISST product period 1979-2010

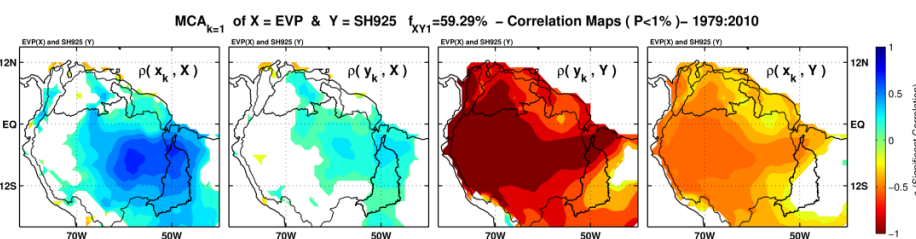
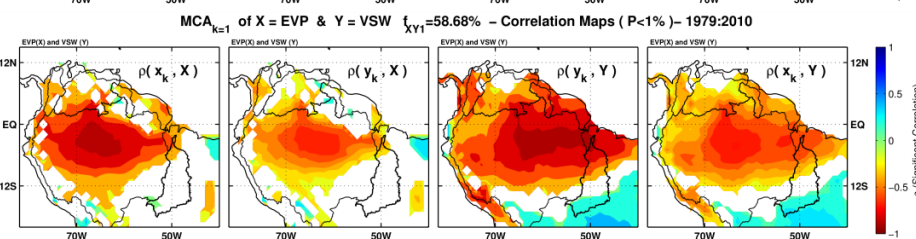
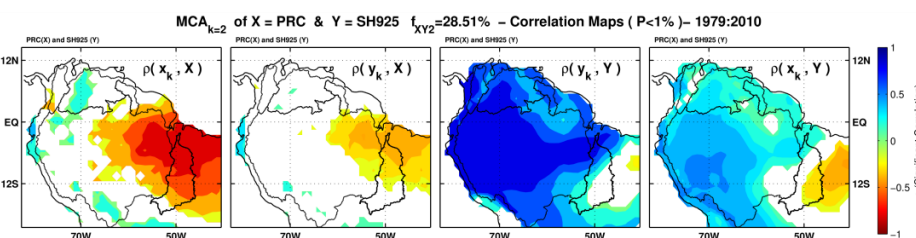
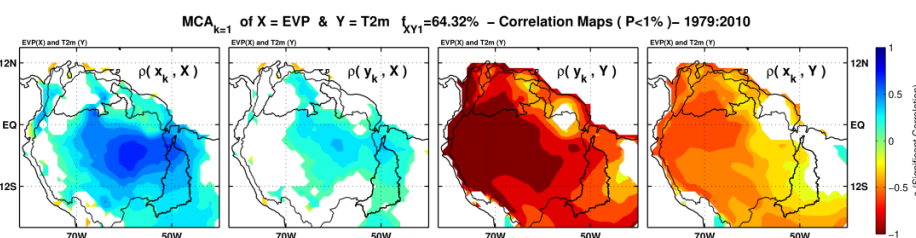
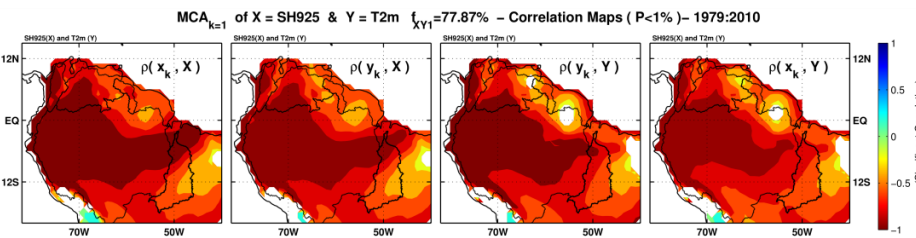


B. Medium ENSO-related MCS₁(PRC, SH⁹²⁵) $f_1^{XY} = 64\%$



C. Low ENSO-related MCS₁(EVP, PRC) $f_1^{XY} = 42\%$



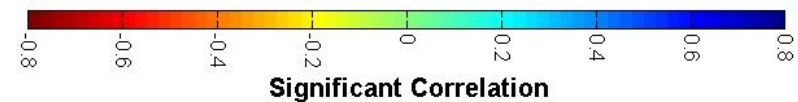
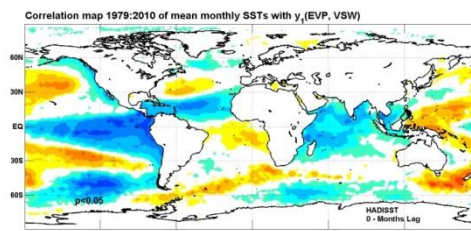
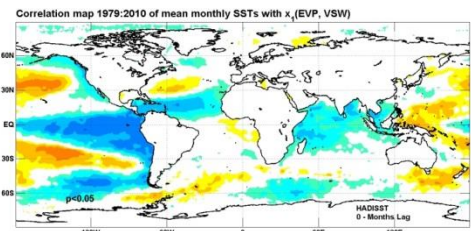


Symbol	Description of map
$\rho(x_k, \hat{Y})$	Correlation between vector x_k with each column vector of matrix \hat{Y}
$\rho(y_k, \hat{X})$	Correlation between vector y_k with each column vector of matrix \hat{X}
$\rho(x_k, \hat{X})$	Correlation between vector x_k with each column vector of matrix \hat{X}
$\rho(y_k, \hat{Y})$	Correlation between vector y_k with each column vector of matrix \hat{Y}

- Type of maps connected with high ENSO related MCS (See SSTs correlation maps at bottom)

- Correlation maps for the pairs SH⁹²⁵-T_{2m} (Continental extent over TropSA), EVP-T_{2m}, PRC-SH⁹²⁵, EVP-VSW, EVP-SH⁹²⁵

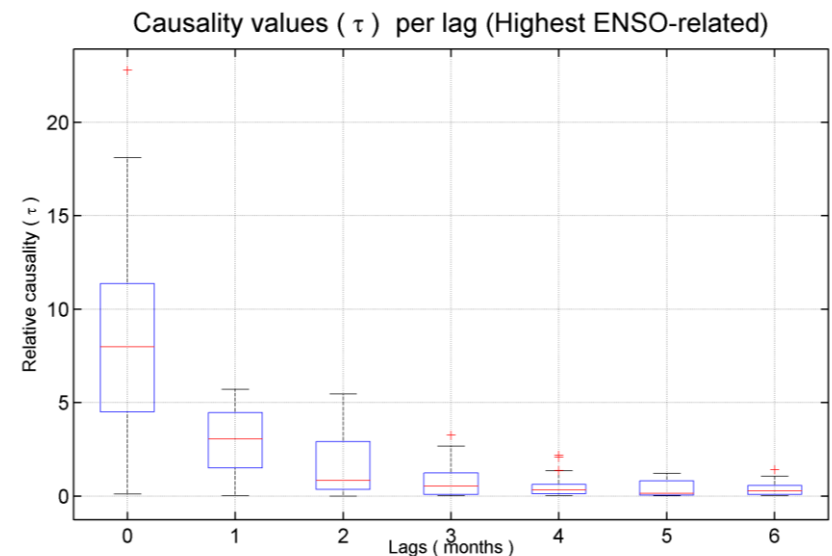
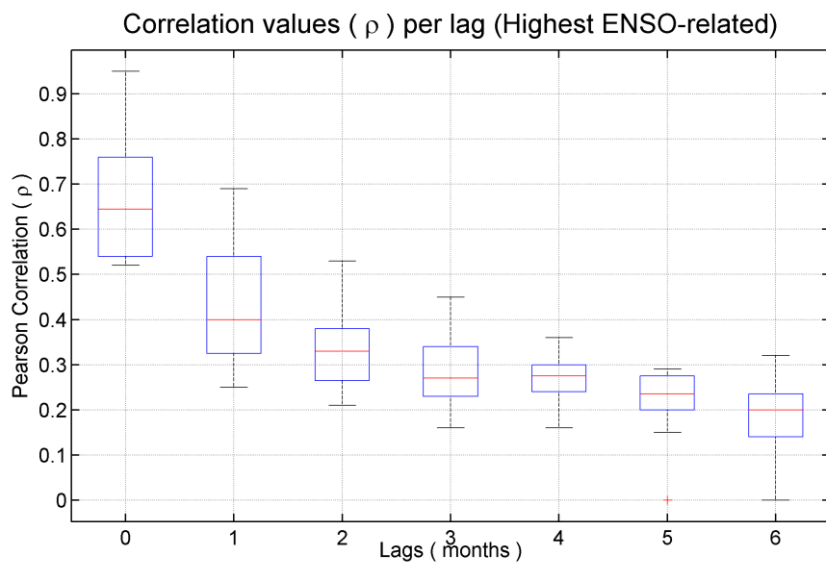
- Generally, continental extent of significant correlations related with pairs including T_{2m} and SH⁹²⁵



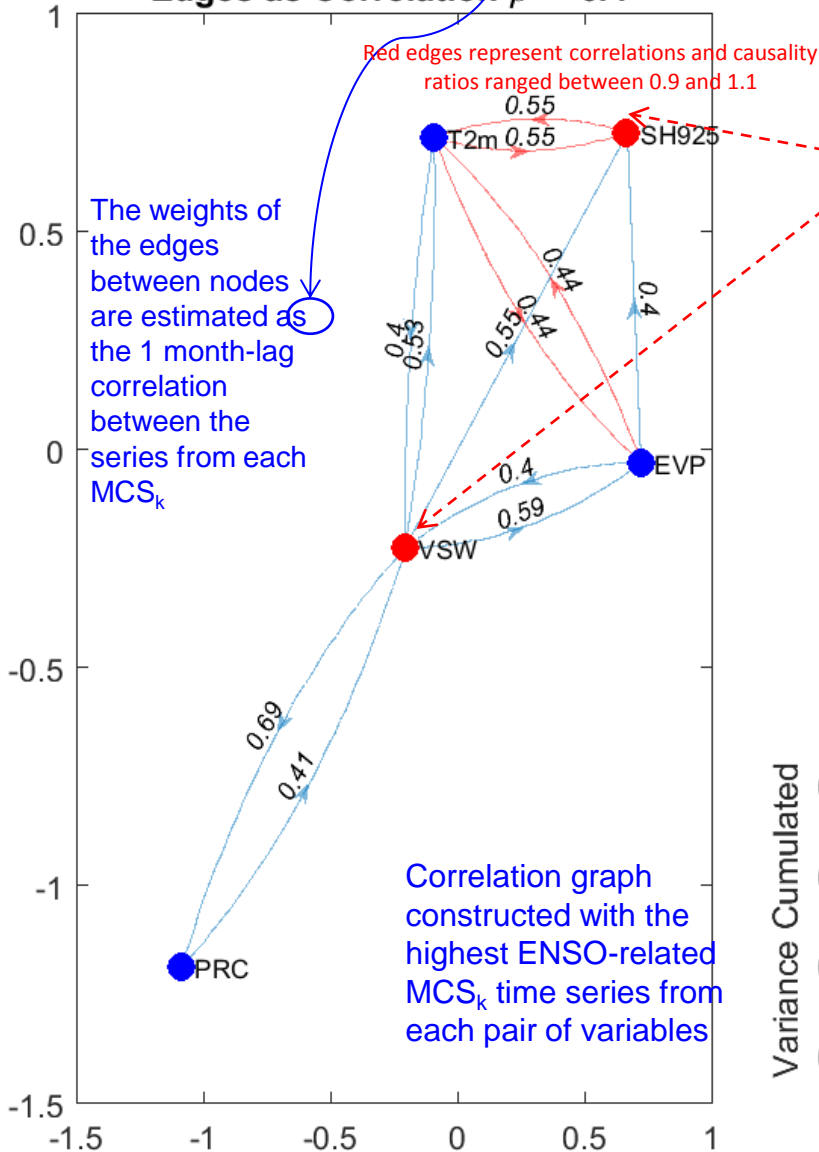
Thresholds to Define Weight of Graphs Edges

- We define a threshold for the edges magnitude to construct correlation and causality graphs.
- This allow us to study the strongest connections among the studied variables.
- In all cases, we select the percentile of 50% of the empirical probability distribution of causalities and correlations for each time lag.

Metric type	Mode	Lag							
		0	1	2	3	4	5	6	
Correlation	Highest	0.64	0.4	0.33	0.27	0.275	0.235	0.2	
Relative Causality (%)	ENSO-related	9.93	4.8	3.44	3.94	2.69	1.75	1.08	



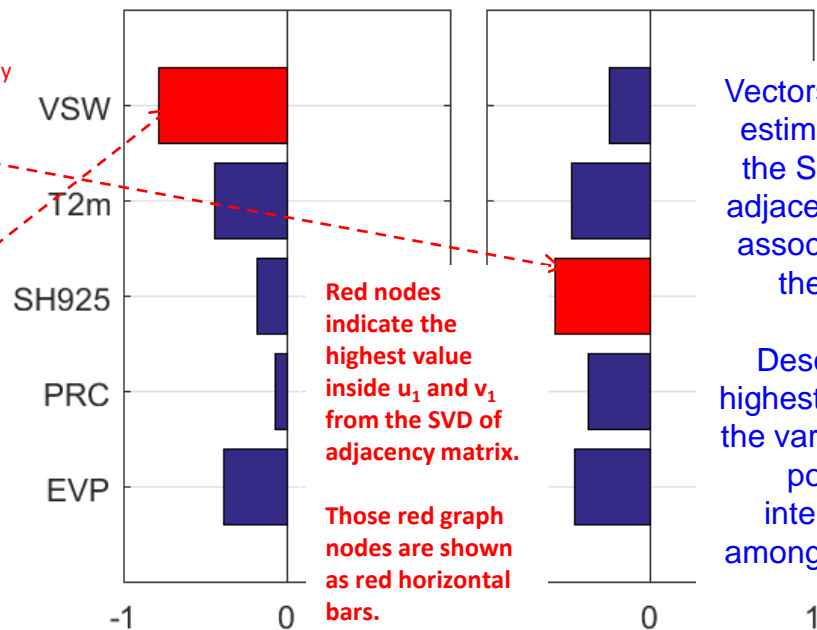
Group 1 of LAF at Tropical South America
Graph Model at lag = 1 Months
Edges as Correlation $\rho > 0.4$



Threshold selected as the median of the empirical probability of all interactions at each lag

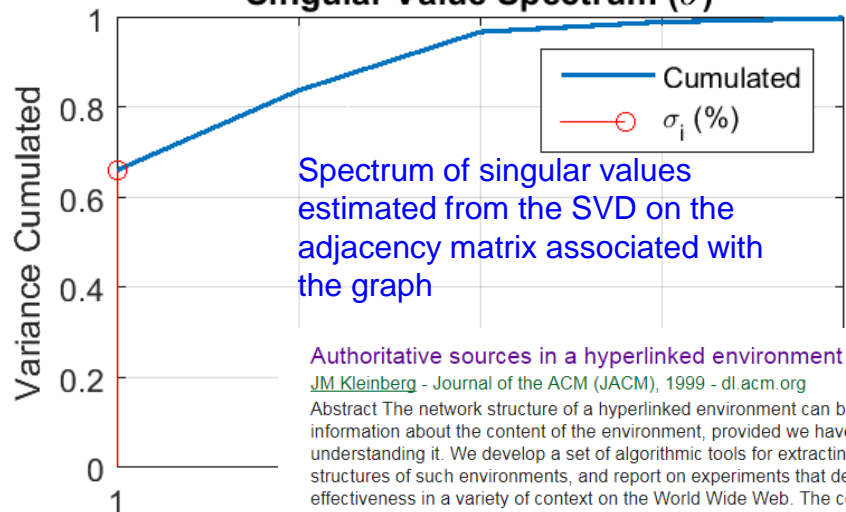
u_1 (Emitter)

v_1 (Receiver)



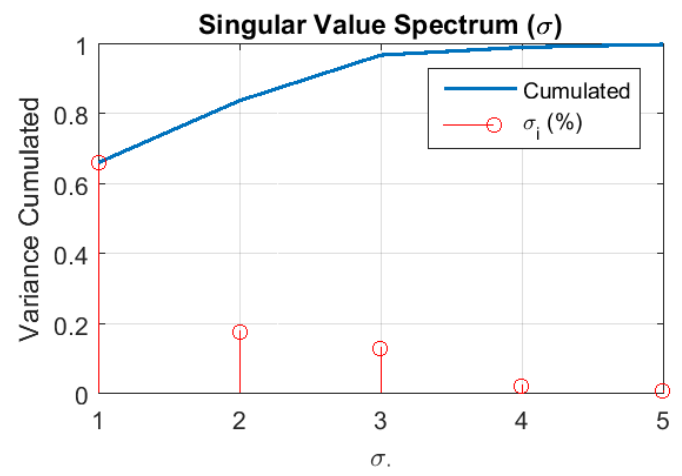
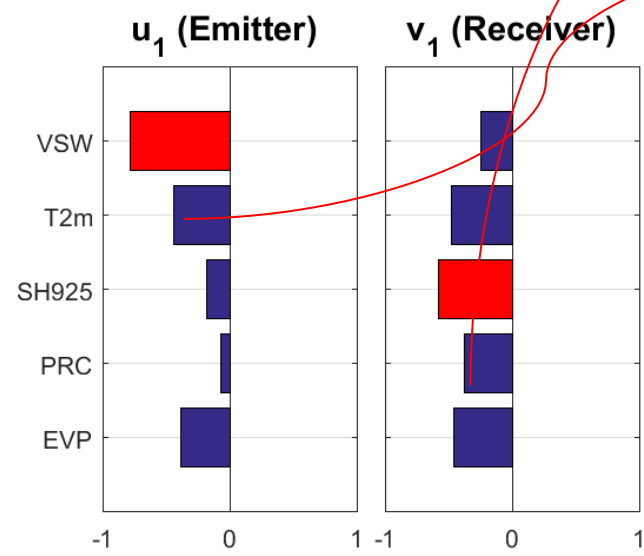
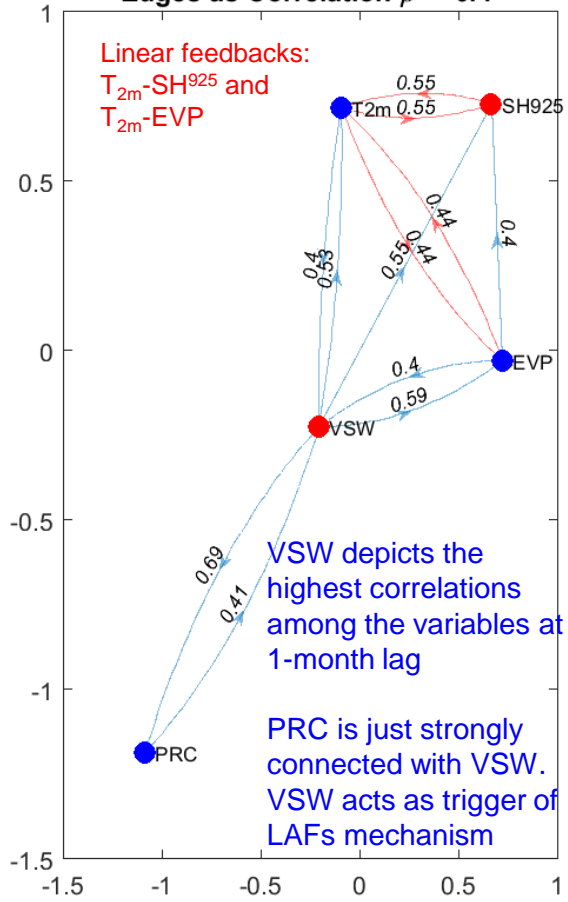
Describe the highest amount of the variance of all possible interactions among variables.

Singular Value Spectrum (σ)



1 lag-month graph using a threshold of significant correlations higher than 0.4 (1979-2010)

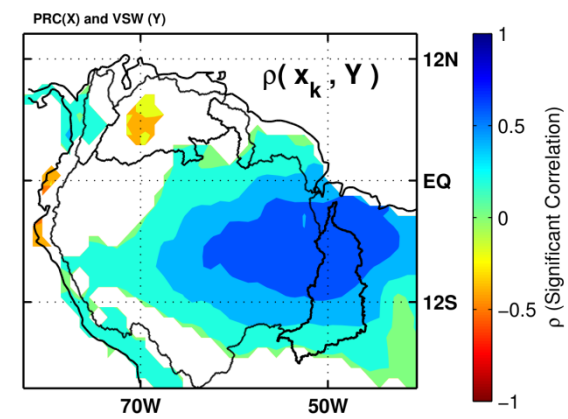
Group 1 of LAF at Tropical South America
Graph Model at lag = 1 Months
Edges as Correlation $\rho > 0.4$



Volumetric Soil Water (best emitter) is essential over Tropical South America to structurally feeds back specific humidity at 925 (**best receiver**) hPa under the group of highest ENSO-related Maximum Covariance States at 1 month-lag for linear metrics.

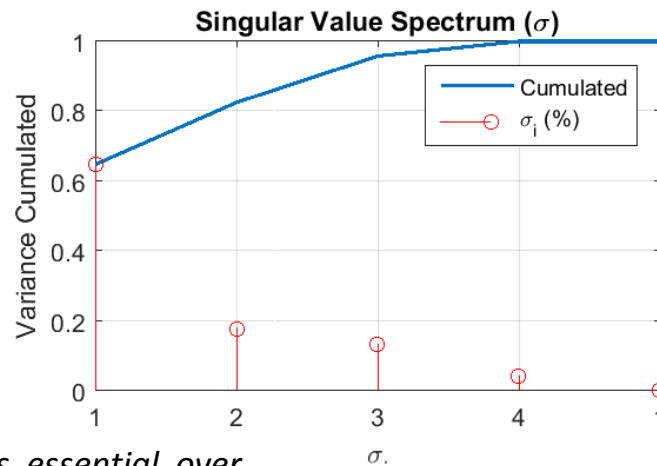
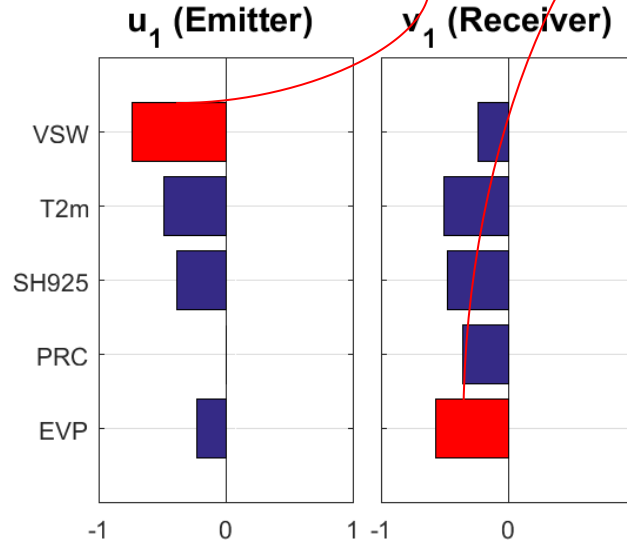
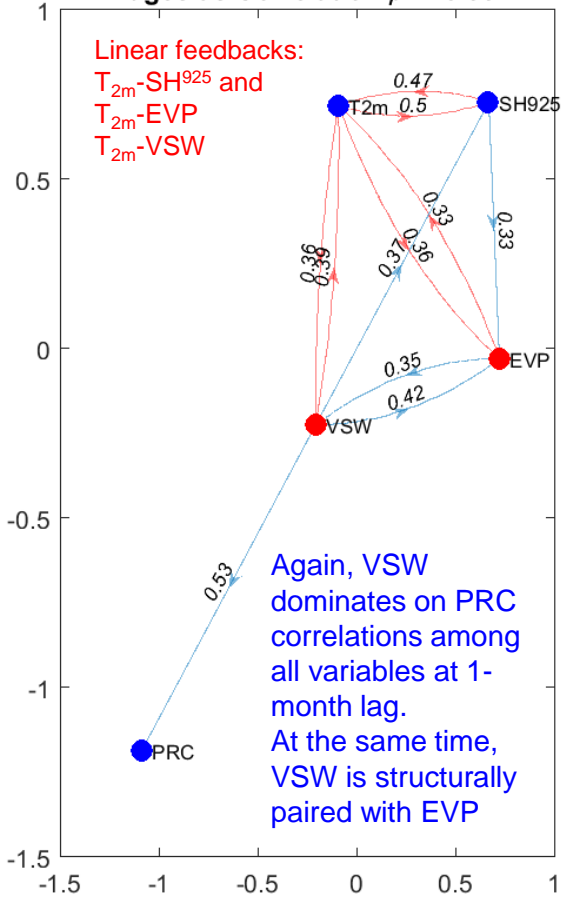
This links structure depicts the Land Atmosphere Feedbacks between state variables VSW and SH⁹²⁵

At 1 month-lag, VSW dominates linear relationships on PRC, EVP, SH⁹²⁵ and T_{2m} at interannual time scales. It remarks the memory of this variable in the context of LAFs over TropSA



2 lag-month graph using a threshold of significant correlations higher than 0.33 (1979-2010)

Group 1 of LAF at Tropical South America
Graph Model at lag = 2 Months
Edges as Correlation $\rho > 0.33$



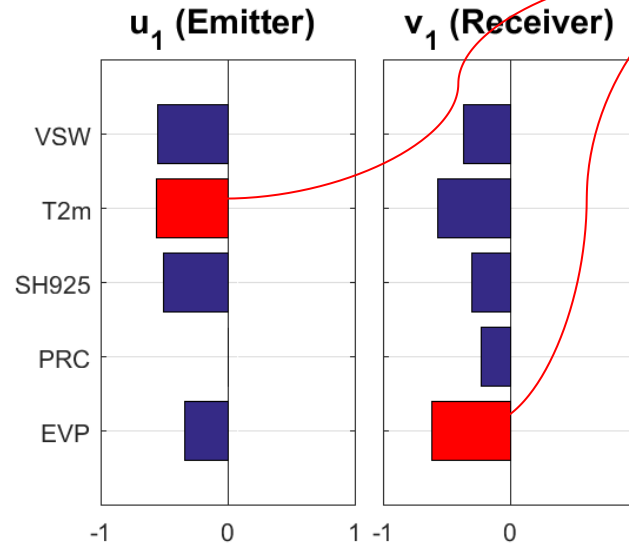
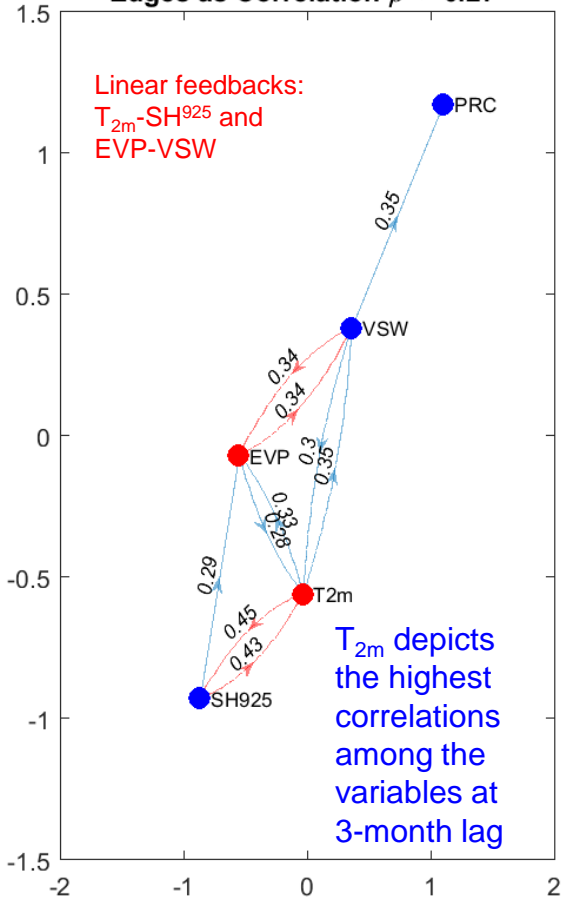
Volumetric Soil Water (best emitter) is essential over Tropical South America to structurally feeds back EVP (**best receiver**) under the group of highest ENSO-related Maximum Covariance States at 2 month-lag

Again, but at 2 month-lag, VSW is essential over Tropical South America to structurally as emitter of group of highest ENSO-related Maximum Covariance States

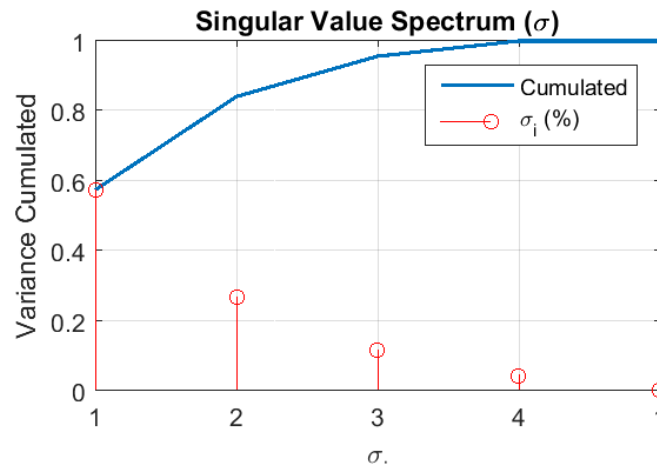
At 2 month-lag, VSW dominates linear relationships on PRC, among EVP, SH⁹²⁵ and T_{2m} at interannual time scales

3 lag-month graph using a threshold of significant correlations higher than 0.27 (1979-2010)

Group 1 of LAF at Tropical South America
Graph Model at lag = 3 Months
Edges as Correlation $\rho > 0.27$



2m Temperature (best emitter) and VSW are essential over Tropical South America to structurally feed back EVP (best receiver) under the group of highest ENSO-related Maximum Covariance States at 3 month-lag.



This links structure depicts the Land Atmosphere Feedbacks between state variable T_{2m} , VSW and EVP

VSW connects PRC feeding back EVP over Tropical South America under the group of highest ENSO-related Maximum Covariance States at 3 month-lag

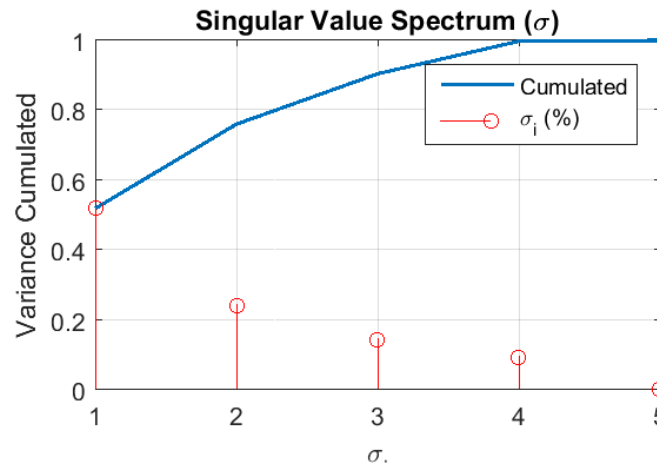
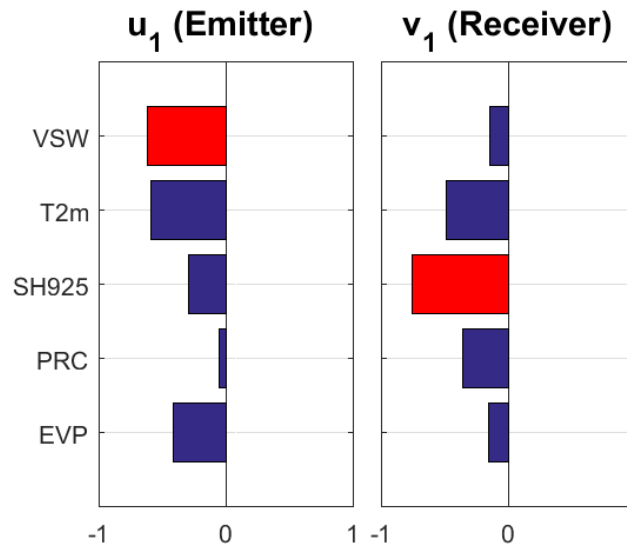
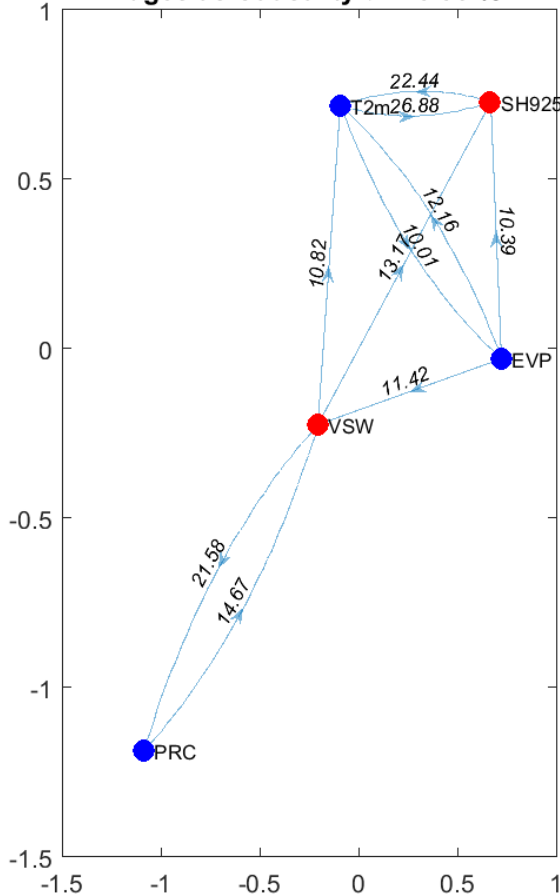
At 3 month-lag, soil humidity dominates linear relationships on PRC, EVP, SH⁹²⁵ and T_{2m} at interannual time scales

Results (3)

Graphs with Non-Linear Edges

0 lag-month graph using a threshold of relative causality higher than 9.93% (1979-

Group 1 of LAF at Tropical South America
Graph Model at lag = 0 Months
Edges as Causality $\tau > 9.93\%$



Volumetric Soil Water (best emitter) is essential over Tropical South America to structurally feeds specific humidity at 925 hPa (**best receiver**) back under the group of highest ENSO-related Maximum Covariance States at 0 month-lag for non-linear metrics .

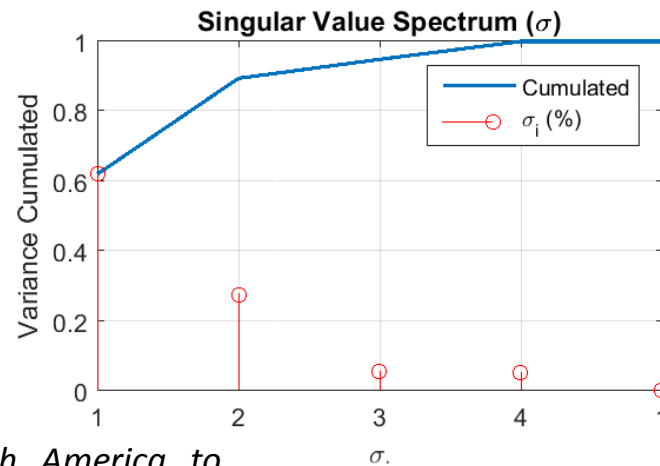
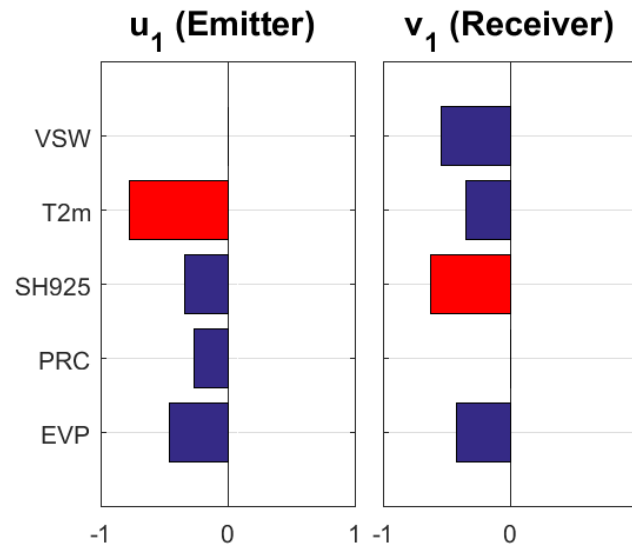
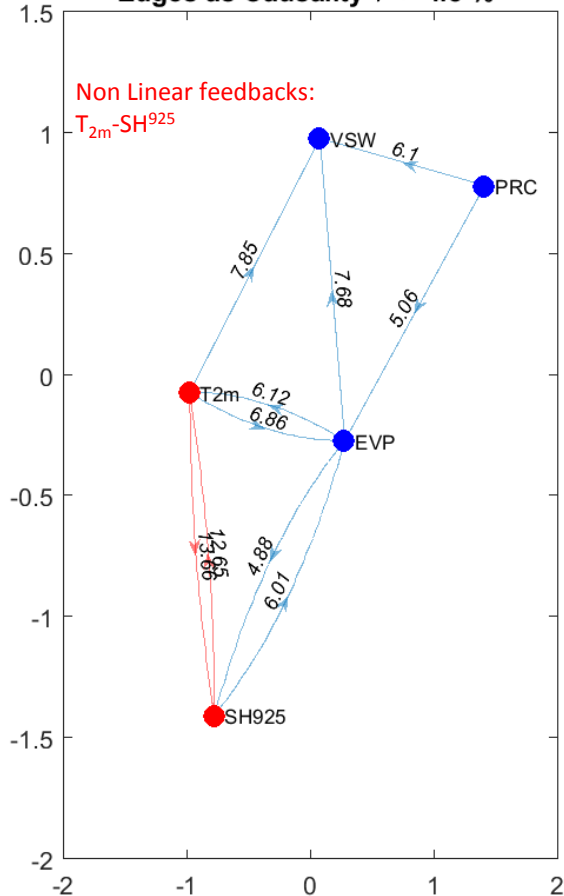
This links structure depicts the Land Atmosphere Feedbacks between state variables VSW- T_{2m} and SH^{925}

VSW is essential over Tropical South America to structurally feeds back SH^{925} under the group of highest ENSO-related Maximum Covariance States at concurrent series (non-linear links)

At 0 month-lag (concurrent), VSW dominates non-linear relationships on PRC, SH^{925} and T_{2m} at interannual time scales. However, EVP dominates on VSW.

1 lag-month graph using a threshold of relative causality higher than 4.8% (1979-

Group 1 of LAF at Tropical South America
Graph Model at lag = 1 Months
Edges as Causality $\tau > 4.8\%$



T_{2m} (**best emitter**) is essential over Tropical South America that structurally feeds back specific humidity at 925 hPa (**best receiver**) under the group of highest ENSO-related Maximum Covariance States at 1 month-lag.

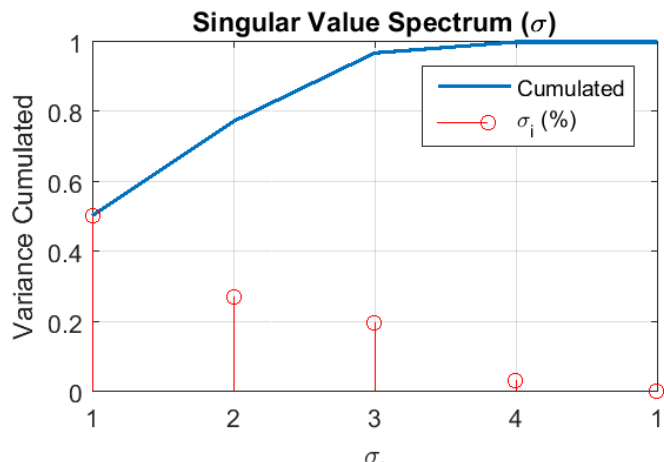
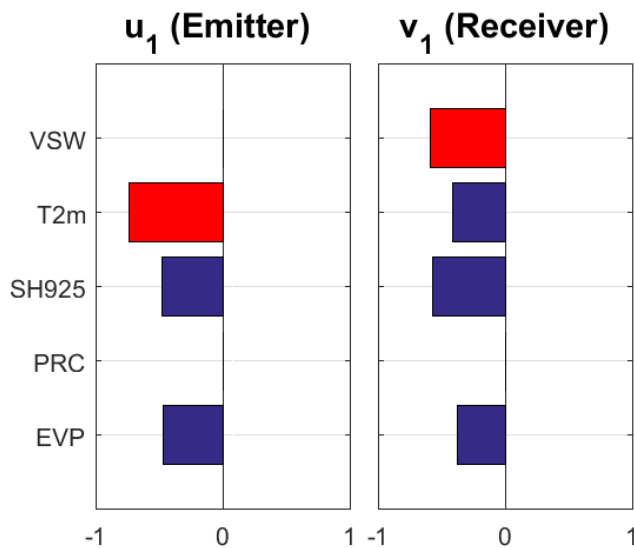
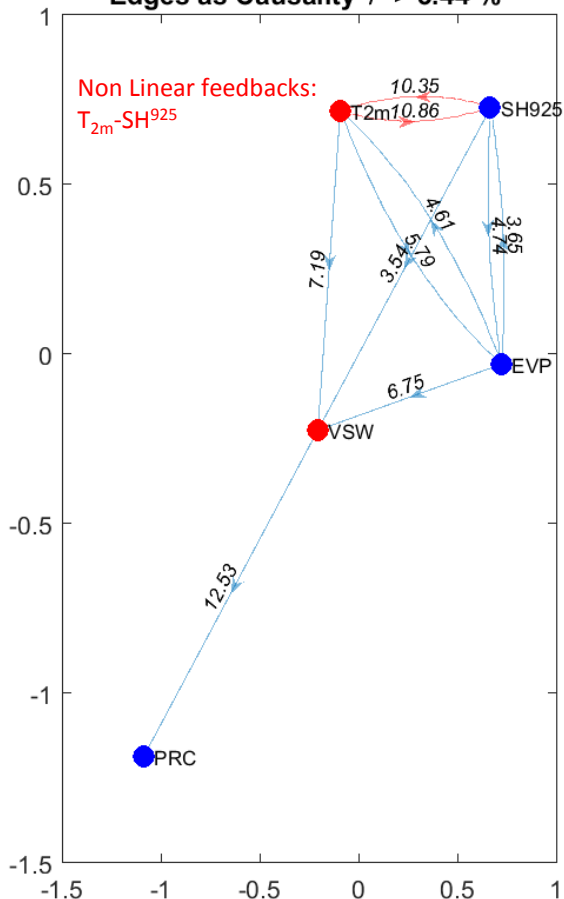
This links structure depicts the Land Atmosphere Feedbacks between state variables T_{2m} and SH^{925}

T_{2m} is essential over Tropical South America to structurally feeds back specific humidity under the group of highest ENSO-related Maximum Covariance States at 1 month-lag

At 1 month-lag, EVP, PRC and T_{2m} dominates non-linear relationships on VSW and at interannual time scales

2 lag-month graph using a threshold of relative causality higher than 3.44% (1979-2010)

Group 1 of LAF at Tropical South America
Graph Model at lag = 2 Months
Edges as Causality $\tau > 3.44\%$



T_{2m} (best emitter) is essential over Tropical South America that structurally feedback VSW (best receiver) hPa under the group of highest ENSO-related Maximum Covariance States at 2 month-lag.

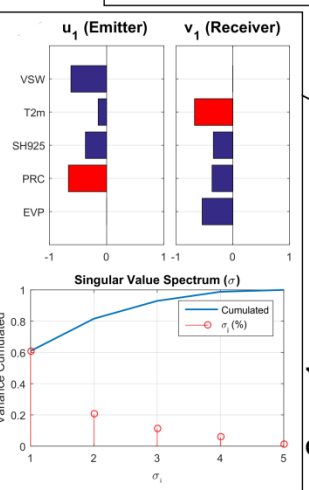
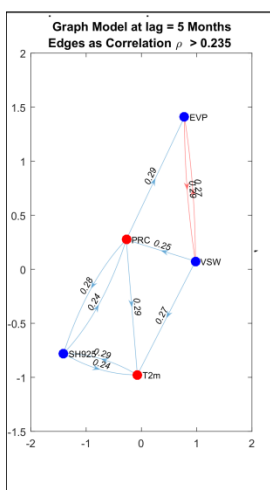
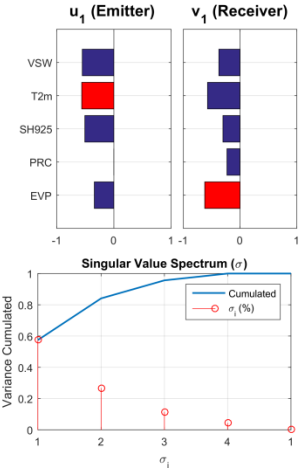
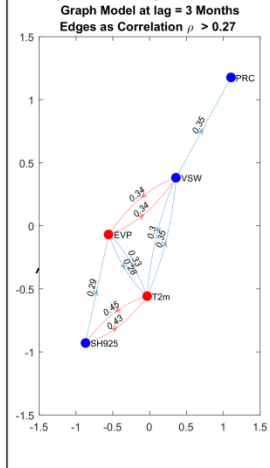
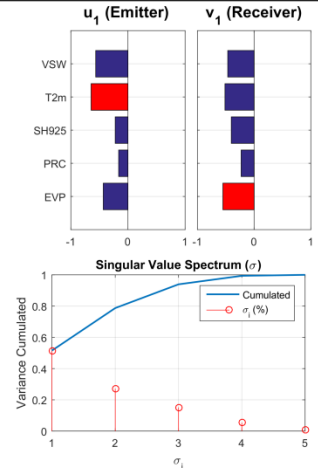
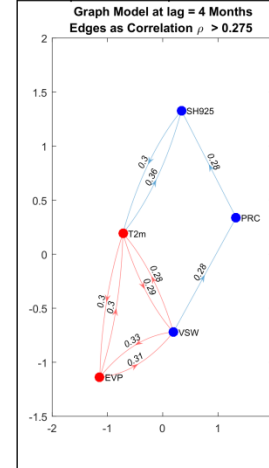
This links structure depicts the Land Atmosphere Feedbacks between state variables T_{2m} and VSW

T_{2m} is essential over Tropical South America to structurally feeds back VSW under the group of highest ENSO-related Maximum Covariance States at 2 month-lag and non-linear links

At 2 month-lag, VSW dominates non-linear relationships on PRC. At the same time, EVP and T_{2m} dominates on VSW at interannual time scales.

Results (4)

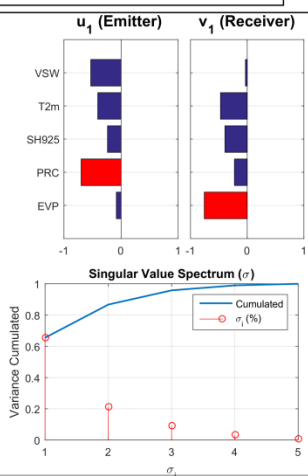
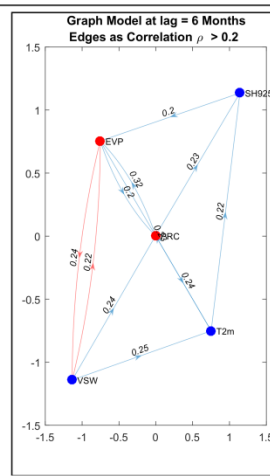
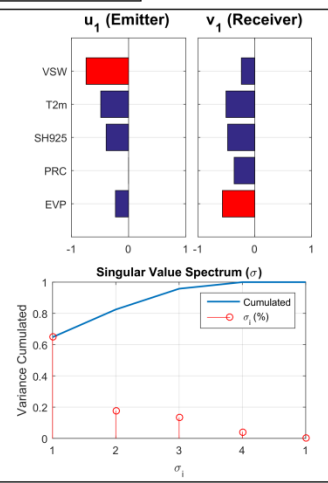
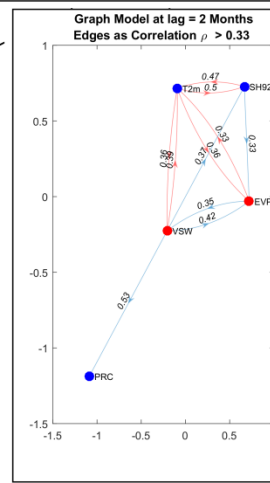
Comparing Graphs with Linear
and Non-Linear Edges



Correlation Graphs Linear Coupling Edges

		t - 6	t - 5	t - 4	t - 3	t - 2	t - 1
SH925	T2m	○	○	○	●	●	●
	VSW	○	○	○	○	○	□
	EVP	○	○	○	○	○	○
	PRC	○	○	○	○	○	○
	T2m	○	○	○	○	○	○
VSW	EVP	○	○	○	○	○	○
	PRC	○	○	○	○	○	○
	T2m	○	○	○	○	○	○
EVP	T2m	○	○	○	○	○	○
	PRC	○	○	○	○	○	○
PRC	T2m	○	○	○	○	○	○
	PRC	○	○	○	○	○	○

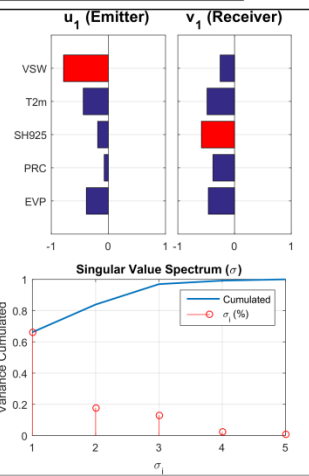
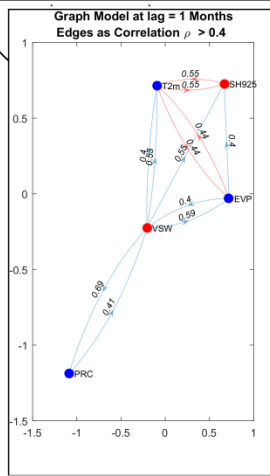
Group 1
High ENSO-related

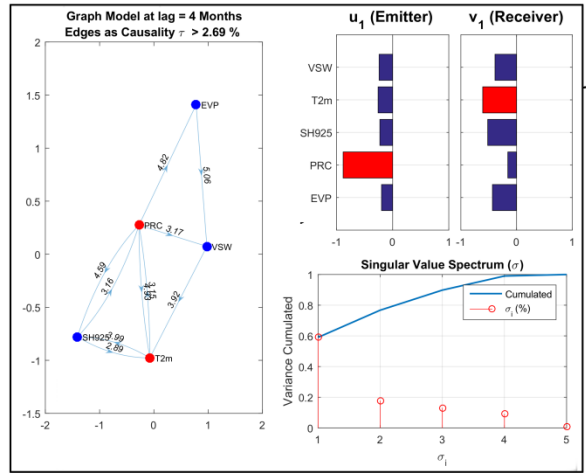
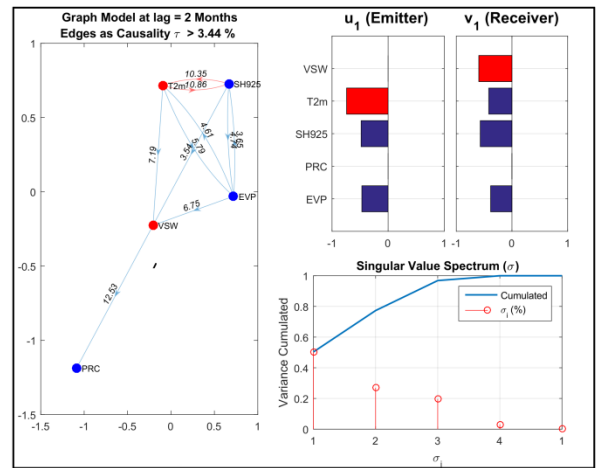
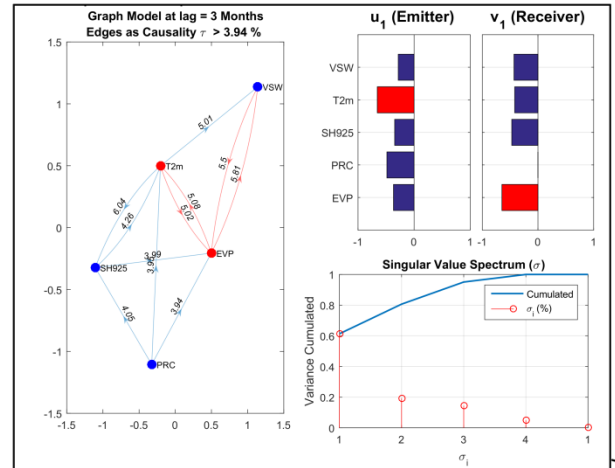


○ Graph's Edge □ Highest Value of main singular vectors u_1 and v_1 per each lag graph

● Edges ratio of correlations or causalities ranging 0.9 - 1.1 per each lag graph

- VSW plays an important role as structural link at several time lags
- VSW provides the memory of the atmosphere-driven processes and their subsequent influence

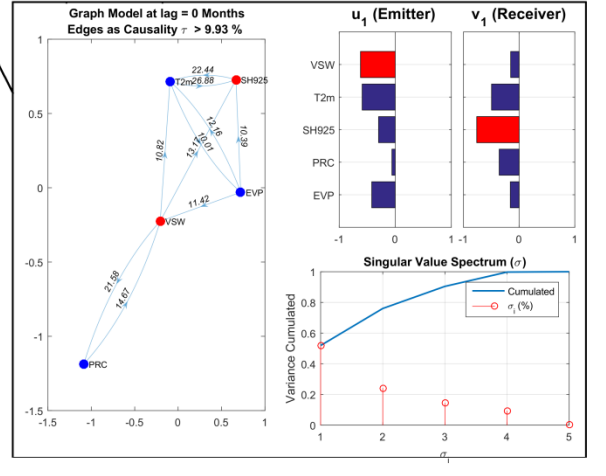
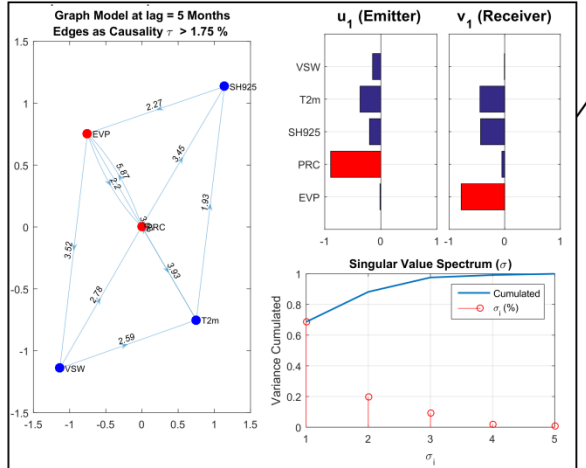
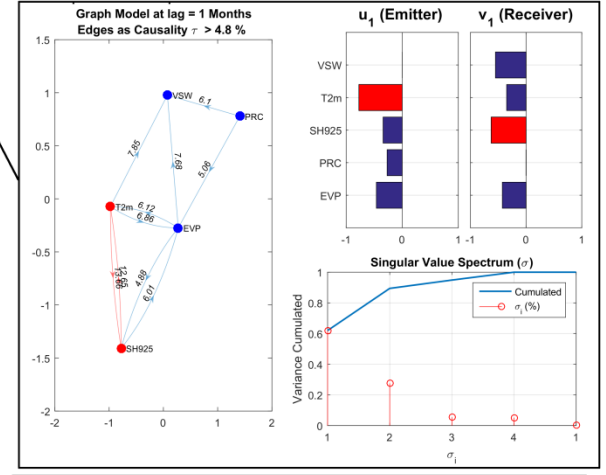




Causality Graphs Non-Linear Coupling Edges

Group 1 High ENSO-related

	t - 6	t - 5	t - 4	t - 3	t - 2	t - 1	t
SH925	<input type="radio"/>	<input type="radio"/>	<input type="radio"/>	<input type="radio"/>	<input checked="" type="radio"/>	<input checked="" type="radio"/>	<input type="radio"/>
VSW	<input type="radio"/>	<input type="radio"/>	<input type="radio"/>	<input type="radio"/>	<input checked="" type="radio"/>	<input type="radio"/>	<input type="radio"/>
EVP	<input type="radio"/>	<input type="radio"/>	<input type="radio"/>	<input type="radio"/>	<input type="radio"/>	<input type="radio"/>	<input type="radio"/>
PRC	<input type="radio"/>	<input type="radio"/>	<input type="radio"/>	<input type="radio"/>	<input type="radio"/>	<input type="radio"/>	<input type="radio"/>
VSW	<input type="radio"/>	<input type="radio"/>	<input type="radio"/>	<input type="radio"/>	<input type="radio"/>	<input type="radio"/>	<input type="radio"/>
EVP	<input type="radio"/>	<input type="radio"/>	<input type="radio"/>	<input type="radio"/>	<input type="radio"/>	<input type="radio"/>	<input type="radio"/>
PRC	<input type="radio"/>	<input type="radio"/>	<input type="radio"/>	<input type="radio"/>	<input type="radio"/>	<input type="radio"/>	<input type="radio"/>
EVP	<input type="radio"/>	<input type="radio"/>	<input type="radio"/>	<input type="radio"/>	<input type="radio"/>	<input type="radio"/>	<input type="radio"/>
PRC	<input type="radio"/>	<input type="radio"/>	<input type="radio"/>	<input type="radio"/>	<input type="radio"/>	<input type="radio"/>	<input type="radio"/>
PRC	<input type="radio"/>	<input type="radio"/>	<input type="radio"/>	<input type="radio"/>	<input type="radio"/>	<input type="radio"/>	<input type="radio"/>
T2m	<input type="radio"/>	<input type="radio"/>	<input type="radio"/>	<input type="radio"/>	<input type="radio"/>	<input type="radio"/>	<input type="radio"/>



○ Graph's Edge ◻ Highest Value of main singular vectors u_1 and v_1 per each lag graph

● Edges ratio of correlations or causalities ranging 0.9 - 1.1 per each lag graph

Conclusions

- The regulatory action of ENSO sets in a stronger memory and resilience of interactions among state and process variables. VSW is a key variable in defining the spatiotemporal patterns of PRC and EVP in TropSA at interannual timescales, and as such plays a major role in regulating LAFs at interannual timescales.
- We defined the dominant LAF spatiotemporal patterns by a pair-wise categorization of variables through Maximum Covariance Analysis (MCA)/Singular-Value Decomposition (SVD), with the aim of quantify the most salient factors associated with ENSO over TropSA. With such patterns, we evaluated the relational structure between state (T_{2m} , SH^{925} , and VSW) and process (PRC and EVP) variables using Graph Theory.
- The identified structure of correlations (linear) among variables differs from that derived from causalities (non-linear).
- Among the studied variables, T_{2m} and VSW exhibit the highest amount of linear feedbacks (correlation) including the one among them at 1 month-lag, and with process variables PRC and EVP.
- For both the simultaneous and lagged analysis, surface temperature (T_{2m}), as a state variable, activates non-linear associations with atmospheric moisture (SH^{925}) and soil moisture (VSW) among the high ENSO-related graphs (causality graphs).
- Under the ENSO influence, T_{2m} is not only a key variable to diagnose the dynamics of interannual LAFs but also has a substantial role on the dynamics and thermodynamics of the lower troposphere and soil interfaces over TropSA